The architecture of the Great Pyramid's lower northern shaft.

Abstract

In the summer of 2021 a series of static images which were taken in 2002 inside the lower northern shaft of the Great Pyramid of Giza were released to the public. In this paper I analyse those images and from that analysis deduce the linear and angular construction parameters of the shaft. I show that the shaft contains a series of rotations around its longitudinal axis which conform to a logical system and that this logical system can be used to extract mathematically precise angular measurements because the system uses known geometric principles.

From the analysis of the shaft's design I show that the metal rods that are located inside the shaft are an original part of the pyramid's construction and explain how one of the two rods was used as a spring mechanism to release a side door within the shaft, behind which was contained a 7cm diameter stone ball that rolled out of the shaft in 1872. Furthermore I explain how the act of investigating this shaft by poking rods up the shaft's incline triggered this spring mechanism to operate.

By using the geometric angles derived from the shaft's construction I show that the stone ball is a model of the Earth and that by solving the mathematics puzzle that the shaft contains, an exact value for the axial tilt of the Earth can be obtained. I then use Laskar's astronomy formula for calculating axial tilt from a known date in reverse to determine the astronomical event date that corresponds to the tilt angle of the shaft and thereby determine that the Great Pyramid of Giza contains an astronomically correct model of the Earth at the winter solstice of 2729 BCE. I show that the values obtained from the pyramid's geometry conform to modern ephemeris data within the error margins of that modern data.

Finally, I show that the building contains a model of the Earth's orbit around the sun, and that the semi major axis of this orbit, the astronomical unit, is specified precisely in architecture using light seconds in a relativistic TDB time frame.

ISBN 978-1-7398691-0-6

The architecture of the Great Pyramid's lower northern shaft.

The lower northern shaft of the Great Pyramid, which emanates from the northern wall of the lower "Queen's" chamber of the building, contains a series of lateral bends which have made the robotic exploration of the shaft more complicated than in the other straight shafts of the pyramid. The history of the shaft's exploration dates back to 1872 when the well documented visit of Waynman Dixon resulted in the discovery of a stone ball, small hook and a broken wooden rod, all of which came out of the shaft during his explorations. Because the shaft is only 21cm square[1], it can be concluded that Dixon must have been poking a piece of wood or alike up the shaft in order to gauge its length and angle when he came across these artifacts, as there would have been no other manner in which he could have explored inside the shaft at that date.

The next significant exploration of the shaft was carried out by Rudolf Gantenbrink's Upuaut project[1], and he succeeded in getting a robotic device, which included inclinometers and video cameras, up to the first lateral bend in the shaft at which point he was unable to negotiate the corner, and could only take video footage of the first few meters around the bend. The exploration of the shaft was continued in 2002 by the team of the Pyramid Rover project and, having designed the robotic device to specifically be able to negotiate the corner in the shaft, they were able to traverse the shaft right to the top where they came across a sealed doorway, very similar to that which Gantenbrink had previously found in the lower southern shaft. Whereas Gantenbrink published all of his technical data, the Pyramid Rover team did not include inclinometers in their device as the intention was primarily to get to the top of the shaft, and so there was very little technical data to publish with only the distances along the shaft released to the public. These distances were to the nearest foot (0.3048 meters) and the team did not release the video footage from inside the shaft.

In 2021 the researcher Matthew Sibson tracked down a series of 51 photographs which are still images from the video taken by the Pyramid Rover team, and he published them[2] during the summer months of 2021. They are a treasure trove of information and in this paper, through careful analysis of the images and a study of the engineering that would have been required to construct the shaft, I resolve the purpose of all of the features that are contained within the shaft.

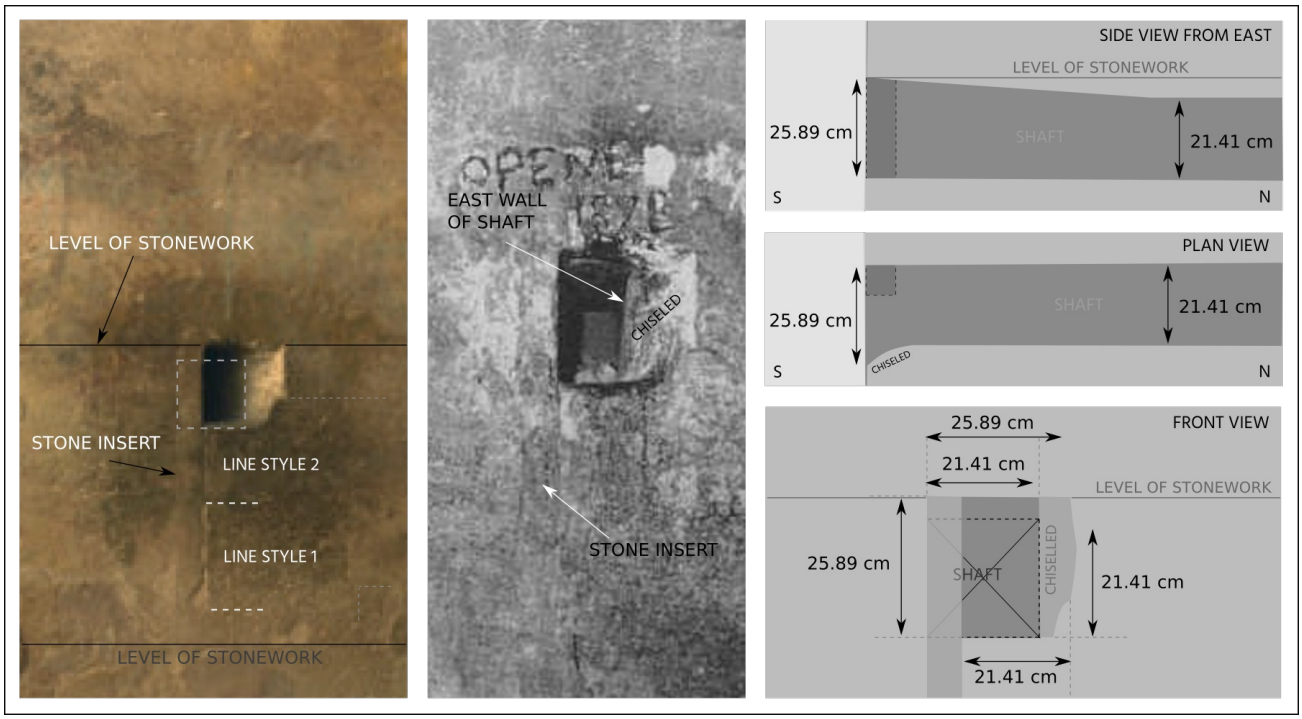

Diagram I-0 - The entrance to the lower northern shaft.

The starting place for the analysis is the shaft entrance in the chamber wall which contains a number of peculiar features which make little sense when first coming across them. Diagram I-0 shows two images of the north wall of the chamber and the shaft entrance along with a cross section through the shaft's north south axis, a plan view and a front view.

The cross section of the shaft at the far northern end of the horizontal section is square and measures 2*n* units in length and height, where *n* is the stack constant determined in a previous paper[3] as being 3/ sqrt(215) cubits, giving 21.4143 cm. On the first image in diagram I-0 the white dashed square marks the location on the wall where the shaft would emerge if it were to continue with this square profile in a north south direction. On both images there is a stone insert to the left of the shaft, the top of which is blocking the left side of the entrance to the shaft. The left edge of this insert and the upper part of the right edge are well formed, and the lower part of the right edge shows distinct recesses and is lighter coloured. On the first image the darker wall markings to the right and below the shaft show a 1 cubit marking on the wall, the bottom right edge of which is clearly defined.

The three technical drawings on the right of diagram I-0 show how the shaft is constructed internally. The roof of the shaft rises at it emerges from the wall and is nearly 4cm higher at the point where it meets the chamber wall than it is at its northern end. The chiseled section, although enlarged by the modern day chiseling of Dixon, is partially original with the lighter areas of stone being the modern day marks, and the darker sections being original in the design. This area is where Dixon spotted a crack in the wall which he then expanded, and not at the vertical side on the left. The front view of the shaft entrance shows how all of the component parts assemble, and it is quite clear that a considerable amount of thought and design work has gone into this shaft opening. Looking casually at the first image it appears that a square shaft hole is present in the wall, when in fact that square opening bears little resemblance to the location of the actual square cross section shaft found deeper in the wall.

This unusual and complex design of the shaft opening is actually the final part of the lower northern shaft's architectural puzzle and will appear again in any analysis of the shaft at the end. By design.

The shaft's side opening

Moving on to the series of photographs from inside the shaft, the most interesting place to start the analysis is with the side hole in the shaft, which appears on photograph 21 in the series of 51 images which shows a side opening on the right side (whilst ascending) of the shaft which has been described as a rectangular hole. Diagram I-1 shows the video still image on the left, and a digitally enhanced version of the image on the right, which has had the contrast and brightness adjusted and the light spectrum graph optimised by one of Sibson's associates.

Diagram I-1 - The side opening in the lower northern shaft (Sibson's door)

Having worked extensively on images of the Unas pyramid in the past, I know not to trust the optical impression that is first obtained when looking at photography inside any of the Egyptian pyramids, and so a geometric analysis of image 21 was constructed as shown in diagram I-2 in which the vanishing point of the images were determined and from these, the shape of the opening in the right wall was established.

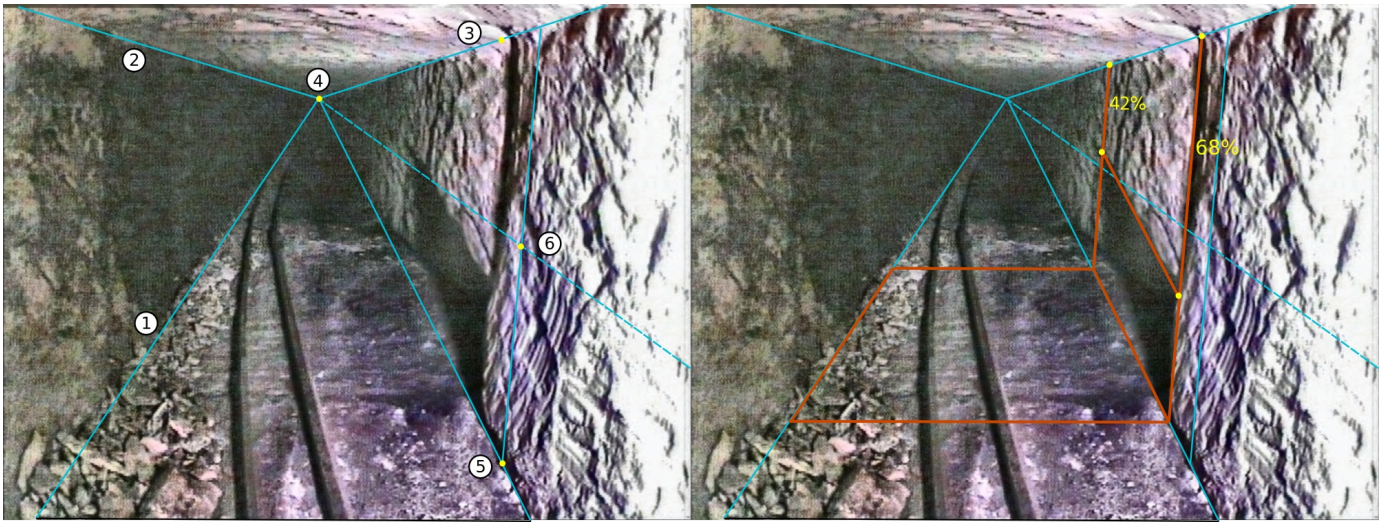

Diagram I-2 - The geometry of Sibson's door

If you look at the original image in diagram I-1 you can see that the joint between the right side wall and the floor is not straight in the section immediately after the opening, and so this bottom right corner of the shaft is not a reliable reference line. Therefore the vanishing point was determined by constructing lines 1,2 and 3 on diagram I-2, the vanishing point 4 was determined, and then point 5 was connected to point 4, giving a true shaft line on the bottom right side. A vertical line was then projected up from point 5 to the roof, parallel to the vertical side line of the door hole in order to remove any perspective distortions, and then point 6 was determined through measurement as being the mid-height point of the right wall. Connecting point 6 back to the vanishing point gives the bisector line of the right wall running up the length of the shaft. The orange lines on diagram I-2 show the verticals of the door hole and, when run across the floor of the shaft, the clearly square shape of the floor of the shaft that is marked out by the vertical limits of the door hole.

From this analysis it can be concluded that the Sibson's side door has a sloping roof with the proportions as shown on diagram I-2, and that the side hole is set into a square section of the right side wall, because the shaft's cross section is known to be square from the measurements taken by the robotics teams who have explored it, and so the square floor section marked in orange must equate to a square side section.

A 3D model of the shaft was then constructed, and diagram I-3 shows the 21.4 cm square shaft viewed from behind the left wall (ascending) of the shaft with the left wall of the shaft and roof cut away, any rotations of the shaft removed, and the image taken perpendicular to the plane of the shaft's side walls. The side door opening's sloping roof is clear to see in this illustration, and the impression that it is rectangular in the photography taken from the robots is a trick of the eye.

Diagram I-3 - The cross section profile of the side shaft opening

There are two very interesting facts which immediately appear from correctly working out the shape of the side hole. This side hole is clearly a doorway in the shaft, and we know from Gantenbrink's robotic exploration of the lower southern shaft exactly what the end door looks like in that shaft. Diagram I-4 shows a close up of the side door in the lower northern shaft and Gantenbrink's door, side by side and to the same scale.

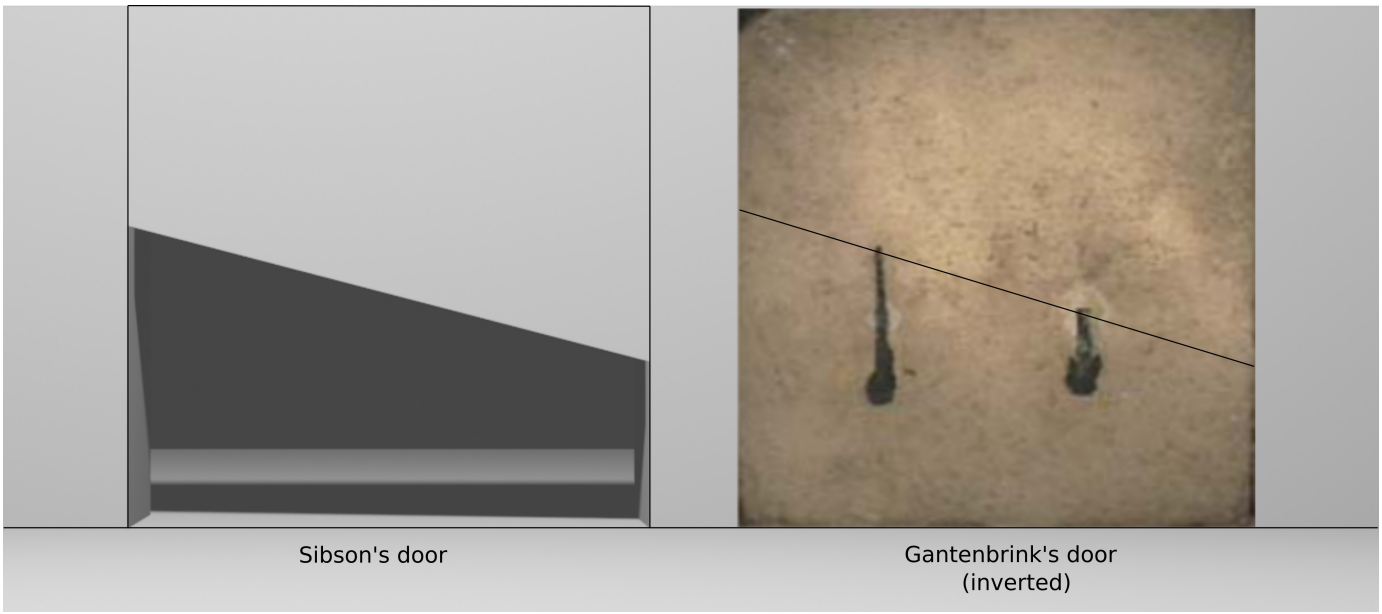

Diagram I-4 - The side door of the lower northern shaft (Sibson's) and the end door of the lower southern shaft (Gantenbrink's)

Within the error margins of the photo interpretation just carried out, the slope of the top of Sibson's door and that of Gantenbrink's door metal 'handles' is the same, showing that the doors are of similar design, noting *importantly* that Gantenbrink's door needs to be inverted. This is a typical feature that can be found within the Great Pyramid's architecture whereby the same concept, but used in the opposite manner, is employed in the construction, and this principle will become relevant again later in this paper.

The second property of the side door in the lower northern shaft is that it is the only location in the whole length of this shaft where the stone ball discovered by Dixon could have been originally located. The ball is currently in the British Museum[4] with object reference EA67818 and the diameter is listed as being 6.5 - 7.5 cm. If this ball is created in the 3D modeling programme with a diameter of 7 cm, or one third of the shaft's height, then in fits into the shaft side hole as shown in diagram I-5.

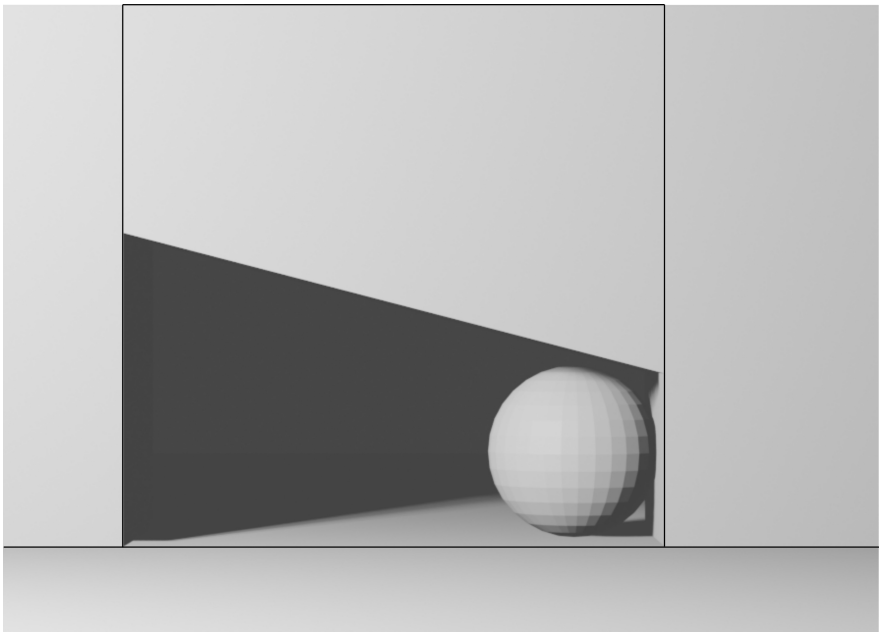

Diagram I-5 - The stone ball located in the side shaft opening

The bend in the shaft

The most remarkable of all the photographs taken from the Pyramid Rover robotics expedition is image number 8 which is shown in its raw and enhanced versions in diagram I-6 and which shows the first bend in the shaft, the point at which Gantenbrink's Upuaut robot was unable to navigate around the corner.

Diagram I-6 - The first bend in the lower northern shaft.

This image contains a wealth of information that is not immediately apparent when first looking at it, and to understand the first point it is necessary to refer to the work that Gantenbrink performed in the *upper* northern shaft of the pyramid.

When Gantenbrink surveyed the upper northern shaft, he measured the inclination and vertical rotation angle of the shaft sections that are located in the tunneled out section of the upper northern shaft directly behind the north wall of the upper chamber. His website is no longer online, but from reference copies that were taken in the past it is possible to display his 3D drawing of this section of the shaft and reproduce the comments that he made in reference to the architecture. Diagram I-7 shows a section of Gantenbrink's CAD drawing of the bends in the shaft sections. The note on the diagram has been added by me.

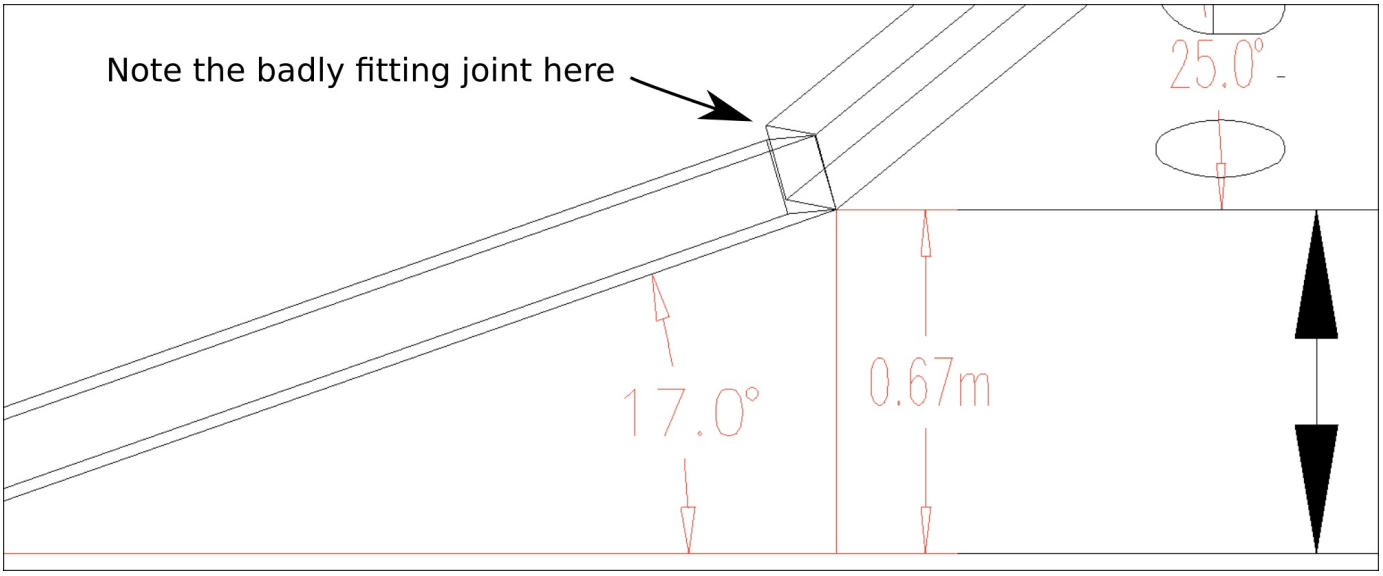

Diagram I-7 - Gantenbrink's analysis of the upper northern shaft.

Gantenbrink commented "*The master builders of ancient Egypt were totally out of their element when it came to constructing this shaft sequence.....they didn't have even a vague notion of how to apply the principle of angle bisection to building the shafts*"

When a shaft of consistent angle of climb is rotated around the vertical z-axis, the floor and wall sections of shaft either side of the joint will not align and the floors will appear skewed. In Gantenbrink's drawing the z-axis rotation angle between the two shaft sections sections is 29.5 degrees, and so in the lower northern shaft at the bend point, the misalignment of the shaft sections should be even more pronounced. If you look back at the image in diagram I-6 you can see that the floor sections and walls of the two shaft sections seamlessly integrate with each other.

This is not possible without some highly sophisticated engineering.

What is also of note regarding the comparison between the upper and lower northern shafts is that the lower one being studied, where the shaft corner transition is perfectly solved, must have been built before the upper one, so the architects and builders already knew how to solve the problem when they arrived at the upper shafts, but chose not to implement a solution.

To analyse the problem and thereby determine how the architects have solved it, and from there to be able to study the photography of the shaft for the engineering evidence, it was necessary to build a 3D model of the shaft and its bends.

Constructing a 3D model

The first information that is required for building the lower northern shaft in 3D is the dimensions of it, and in particular the angular rotations, both around the horizontal and vertical axis, that are employed within it. The whole of the shaft's horizontal section which runs south to north from the lower chamber north wall, and the first inclined section that is also aligned to the north-south axis was documented in Gantenbrink's CAD drawings. The linear measurements on the drawing are accurate, but he was unable to obtain a publishable inclination angle due to the fluctuations in the shaft's floor stones from section to section making any average value meaningless.

Petrie measured the inclination of the start of the shaft (the first shaft floor stone) as being 37.5^{o} and when Gantenbrink came to drawing this section of shaft onto his CAD drawing, he drew it at an angle of 43.67^{o}. From my own work analysing the geometry of the building, this section of shaft falls between Petrie and Gantenbrink's values but, as will be explained, the exact value is of no consequence. A nominal average value, between Petrie's and Gantenbrink's, of 40^{o} can be used.

The second angle that is required is the rotation of the second section of shaft around the vertical z-axis, and at the moment there are only two places we can find this from. The first is Gentenbrink's reporting that the shaft bends to the left at approximately 45^{o}, which he has estimated by looking at the footage from inside the shaft from his robotic video. If you refer back to diagram I-6 you can see how he came to this conclusion simply by looking at the image. However, analysis of this image tells a different story, as shown in diagram I-8. On this diagram, the side wall lines of the shaft where they meet the floor have been extended 'into the distance' and then a 3D perpendicular line has been drawn running from the shaft lines to the left. Using a visually calibrated angle measure the right side floor-wall line of the shaft around the bend has been drawn on as a cyan coloured arrow. The angle estimate on the left side is around 65^{o} and the angle estimate from the right side is about 55^{o}.

These angles should be the same, and clearly are not, so there must be some feature in this image that has not yet been identified, and it is by searching for the cause of the disparity between these two angles that the precise angle for the bend can be uncovered in the architecture.

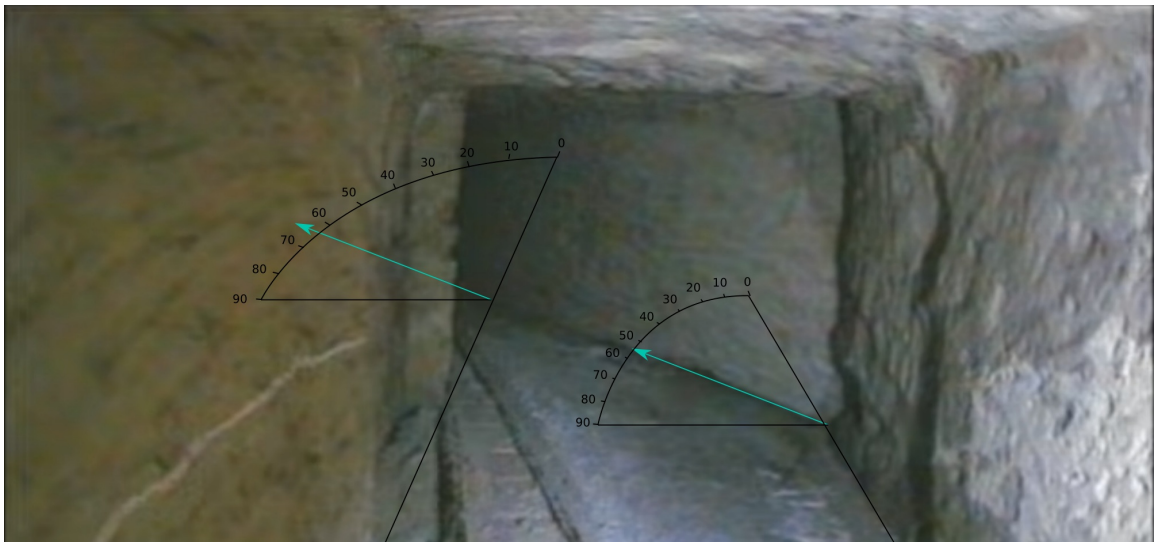

Diagram I-8 - Estimates of the shaft bend angle taken from image 8

You can see from the image in diagram I-8 that the cross section of the shaft at the bend is not a square, but is a rectangle. It can be checked that this is not lens distortion on the robot's camera by comparing the first image in Sibson's series of 51 images with image number eight as shown in diagram I-9.

Diagram I-9 - The cross section of the lower northern shaft at the shaft's first bend point

The cross section of the shaft in the first image is square, and in the second image it is rectangular, and since the image width and height proportions are the same on both photos, it can be concluded that this is not lens distortion and the cross section of the shaft at the bend point is indeed rectangular, with a small rotation of about 1.6^{o} apparent in the images. It is important to compare this to Gantenbrink's published image taken from roughly the same place, where it can be seen that Gantenbrink has artistically distorted his image width to make the shaft cross section at the bend point look square. Gantenbrink's published and distortion corrected image are shown in diagram I-10.

Diagram I-10 - The manipulated image from the Upuaut project, left, and corrected on the right

The next point of note is that at the bend point the left wall of the shaft has an indentation built into it just before the corner, which exposes a section of the left side wall of the shaft that is beyond the bend. This is an intentional architectural feature and not a piece of casual craftsmanship on the part of the builders because it shows how the cross section of the shaft at the corner has been constructed as shown in diagram I-11.

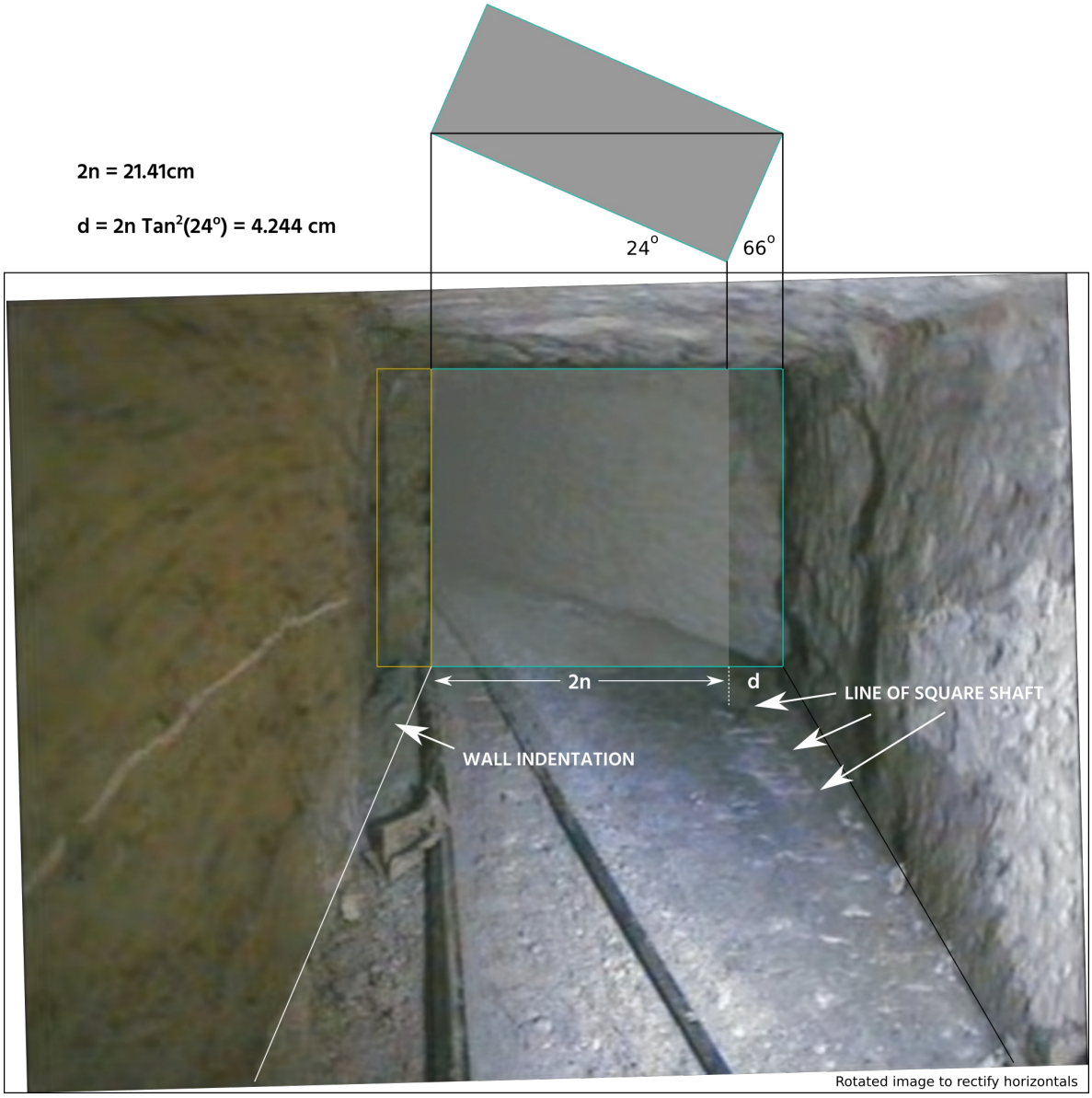

Diagram I-11 - The shaft bend fully resolved with the architects bend angle displayed.

If the square cross section of shaft determined from the shaft height is drawn onto Sibson's image 8 and butted up against the left wall, then the gap on the right of the square shaft cross section, between it and the right wall, is identical in width to the section of protruding wall that has been deliberately exposed on the left. In addition, it is possible to see the line marked on the floor by the architects where the right side of the shaft would have been if the shaft was of a consistent width of 21.4cm. From the geometry, the right wall of the shaft at the corner is 4.24 cm to the right of this, and the shaft width at the bend point is 25.89 cm. These are the exact same measurements that were seen at the entrance to the shaft in diagram I-0.

The reason for the systematic design of the 'side panels' either side of the square cross section becomes apparent when you place a right angled triangle with its hypotenuse horizontal and its corners aligned with the shaft. Its sides are angled by 66^{o} and 24^{o} to the horizontal. Because of the way that the geometry is formed, this is a very sensitive calibration system, and the angle of rotation of the shaft around the z-axis as it turns to the left in the image can be read off with accuracy as being 66^{o}.

This engineering also allows the plan view of the lower section of the shaft to be determined because the width of 25.89 cm at the bend point has been determined. This width expansion explains why the two estimated angles in diagram J8 are different, and is also duplicate architecture to the entrance cross section.

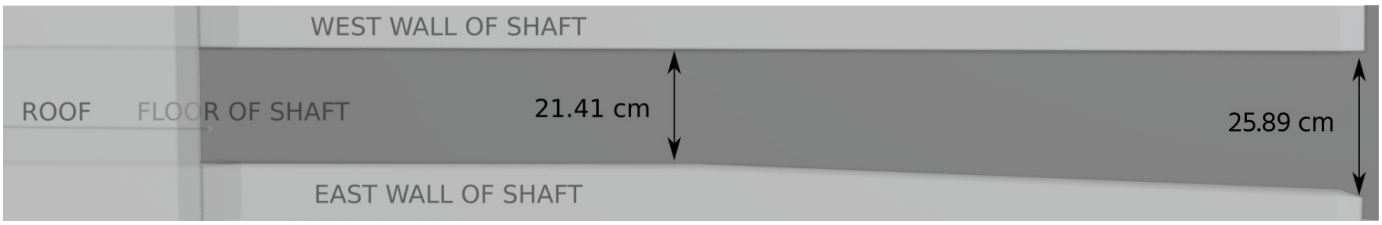

Diagram I-12 - The width expansion at the bend point of the lower northern shaft, with the roof of the shaft removed.

The construction of this bend area raises the question as to why this bend angle in the shaft is so important that the architects would go to substantial lengths in the construction of the stonework to specify it through additional architecture. The answer can be found by building the 3D model of the second section of the shaft and including in that model the gallery room of the pyramid.

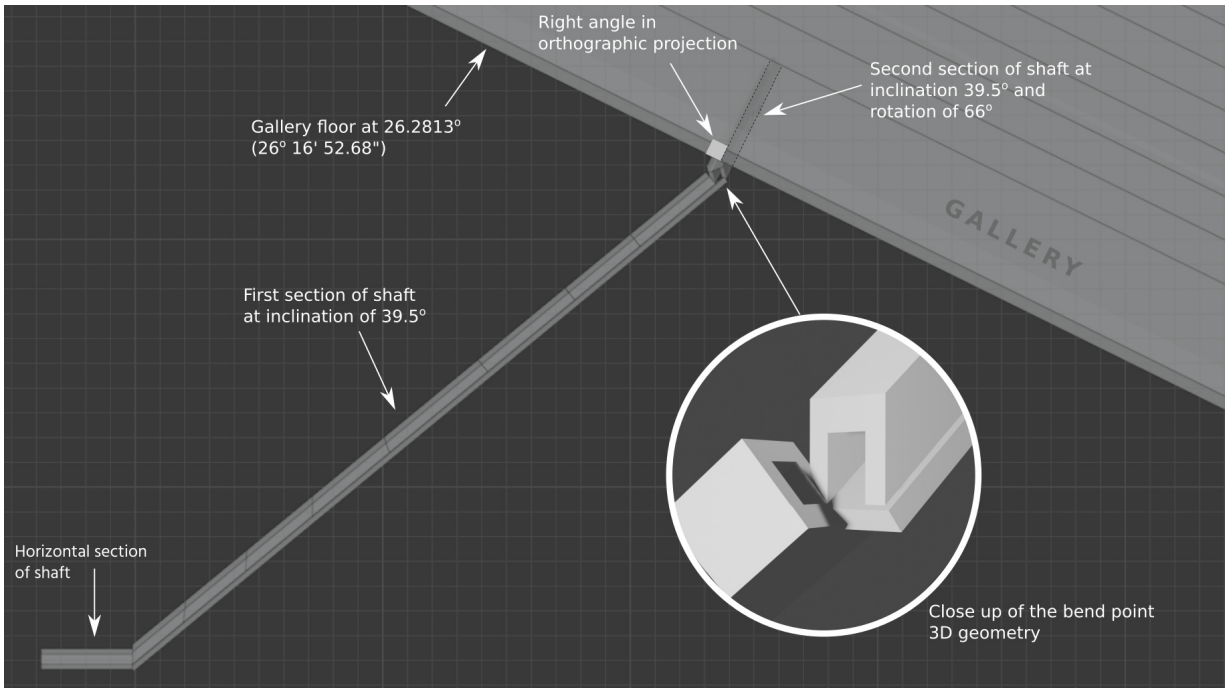

Diagram I-13 - The orthographic projection of the lower northern shaft and gallery floor.

Diagram I-13 shows an orthographic projection rendering taken from due east of the pyramid from a 3D modeling programme ('Blender') with the lower northern shaft angle of incline set at 39.5^{o} and the z-axis rotation of the second section of shaft around the corner set at 66^{o}, and the gallery included in the model.

As can be clearly seen, the second section of the lower northern shaft that passes behind the gallery is perpendicular to the the gallery floor when viewed in orthographic projection, and the systematic design of the architects is revealed. Because the gallery floor angle is known with precision, the exact angle of the bend in the lower northern shaft can now be worked out using 3D trigonometry from the known angle of the gallery and the known angle of the first part of the lower northern shaft, giving the angle of rotation of the second part of the shaft around the vertical z-axis as precisely 66.2394^{o}.

Engineering the joint in the shaft

As can be seen in the inset circle in drawing I-13, joining up the two sections of shaft requires engineering to the highest quality if the joint is to remain smooth and invisible when traversing the shaft, and to understand the remarkable way in which this has been done by the architects we need to return to Gantenbrink's analysis of the shaft stones. He noted that the shafts are constructed with the walls and roof all in one piece, and this 'n' shaped cross section is then laid onto a floor bed, as shown in diagram I-14.

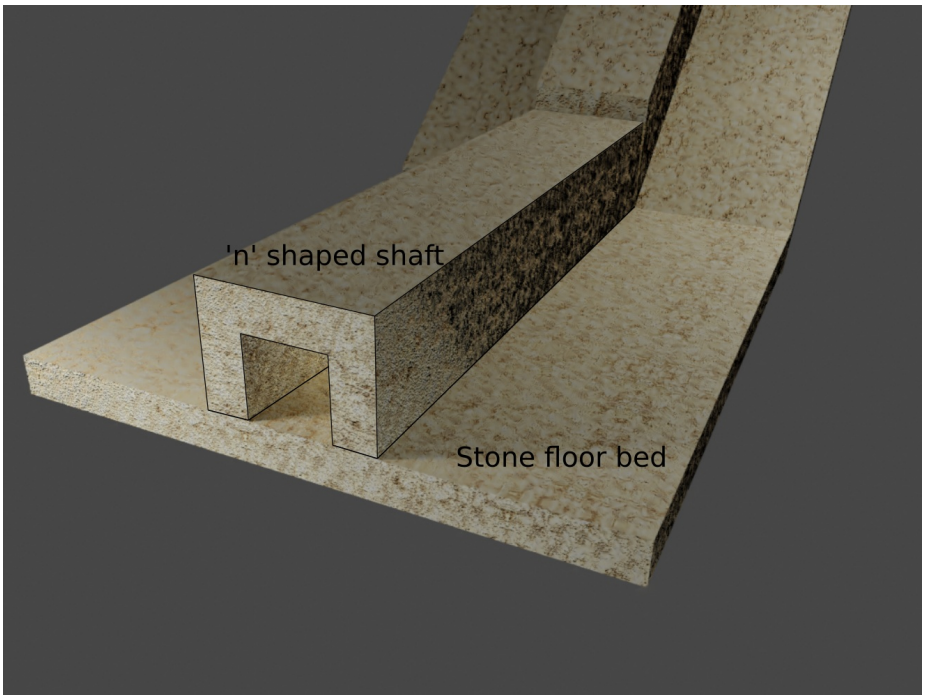

Diagram I-14 - The construction method of the shaft stonework, as explained by Gantenbrink.

We can now look at the bend area of the shaft that is the focus of interest, and see how the first section of the shaft and the second section of the shaft around the bend point interact with each other. The walls and roof do not join up, as was shown on diagram I-13, but what is remarkable is the line of intersection of the two floor planes, which is shown in detail in diagram I-15.

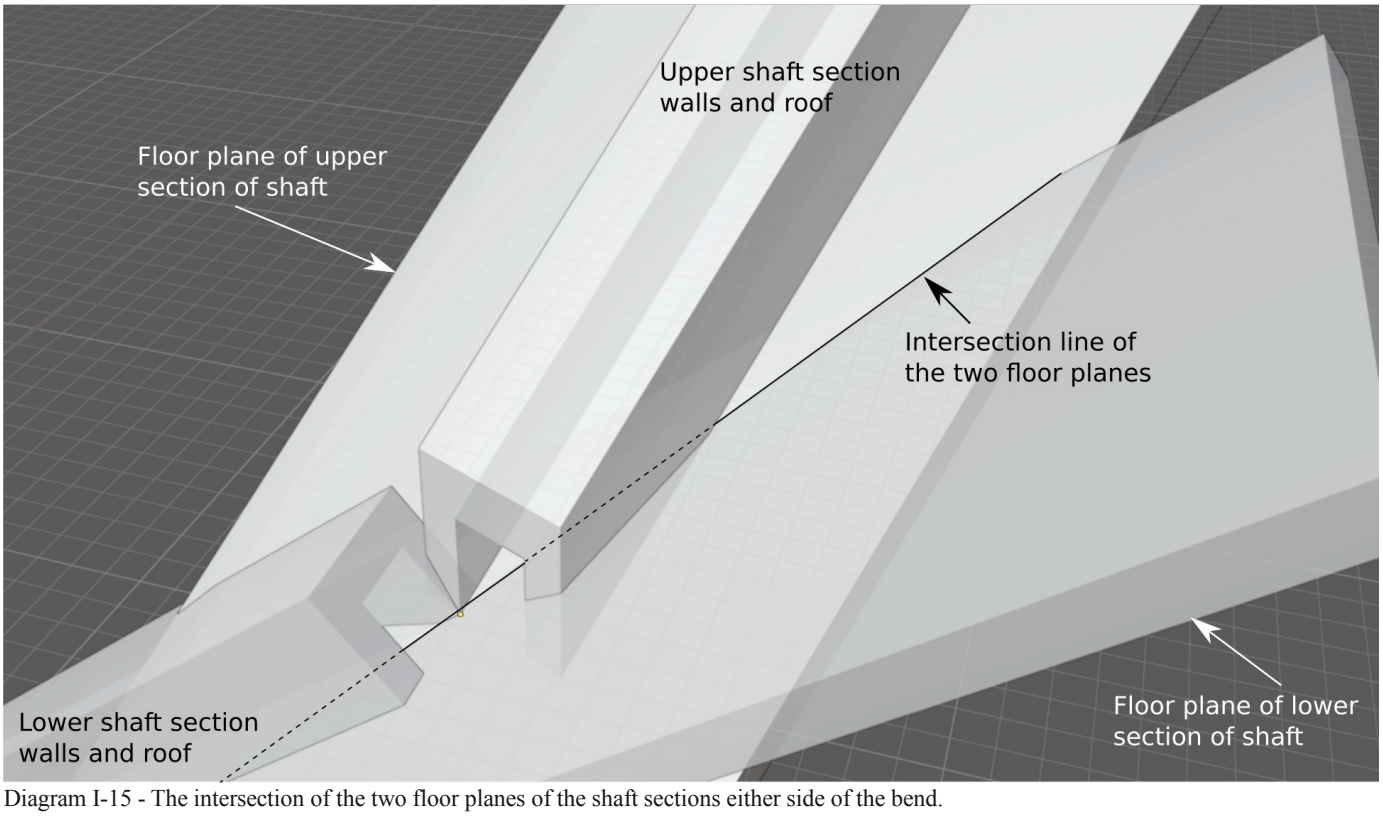

Diagram I-15 - The intersection of the two floor planes of the shaft sections either side of the bend.

The line of intersection of the two floor planes runs along the very same line that the square rod in the shaft follows, and the similarity is such that if, in the 3D model programme, a small square rod of 5mm cross section is placed along the floor plane intersection line and a photograph is taken from inside the lower section of shaft, the image is all but identical to Gantenbrink's, as shown in diagram I-16. The reason that Gantenbrink's image is used in this comparison is that the square rod has since slipped down the shaft a small amount as the various robotics explorations have made their way up the shaft, and so Gantenbrink's image is the only one we have of the undisturbed rod.

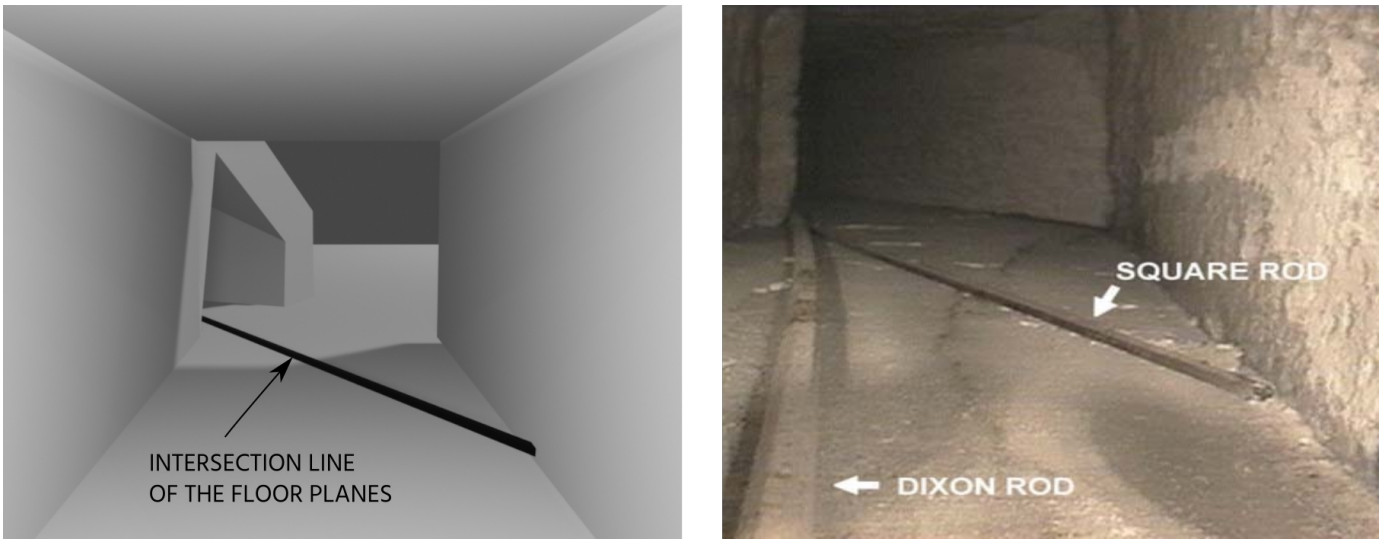

Diagram I-16 - A comparison of the floor plane intersection line and Gantenbrink's image from inside the shaft.

In the rendered image on the left, the unresolved upper section of shaft walls and roof can be seen, but the upper floor section has been removed from the image as it interferes's with the line of sight up the shaft.

Because it is impossible that this square rod could have been put precisely into this position by 'unknown explorers' after Dixon in the late 1800s, positioned as it is on the perfect geometric floor intersect line of the two shaft sections, it has to be concluded that the square metal rod is an original feature of the shaft.

The line of the floor intersection has been used by the architects as the joint between the two floors, and the rod, sitting on this line as it does, hides the transition between the two floor planes at the corner. However, as the left image shows in diagram I-16, the two sections of shaft also require rotating around their respective longitudinal axis in order to match up the floor slopes to make the transition at the corner smooth, and also to preserve the geometry that is shown in diagram I-13.

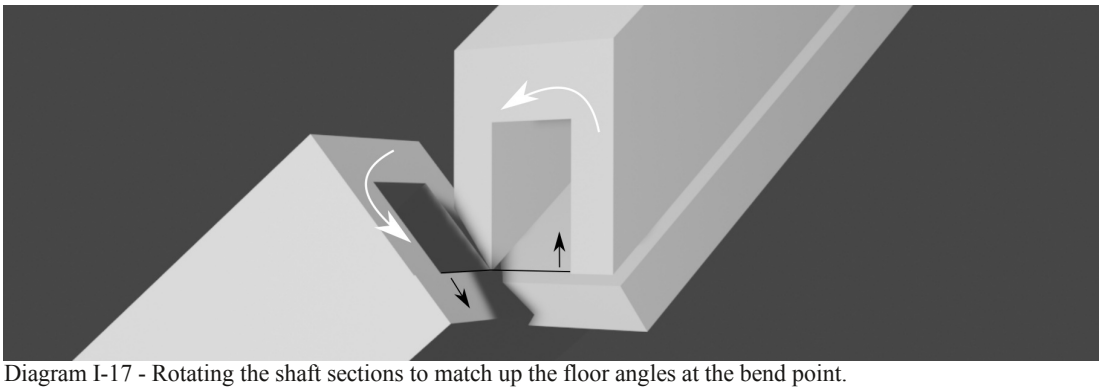
Diagram I-17 - Rotating the shaft sections to match up the floor angles at the bend point.

Diagram I-17 illustrates the rotations that can be used to match up the floor slopes and also preserve the 3D geometry of the shaft in relation to the gallery floor. When looked at from inside the shaft whilst ascending, the first section of shaft can be rotated in a clockwise direction and the second section of shaft in an anti-clockwise direction. The evidence for the rotation of the lower section of shaft has already been seen in diagram I-9 where Sibson's image numbers 1 and 8 both show an angular rotation of about 1.6 degrees which would be almost indiscernible to casual observation when looking into the first section of the shaft from the horizontal section that comes from the lower chamber.

The evidence of rotation in the second part of the shaft around its longitudinal axis is evident in many of Sibson's series of photographs, with diagram I-18 showing the raw and enhanced image of the top of the third section of shaft (Sibson's image number 25). Although this image does not resolve the absolute rotation angle of the shaft sections, it does clearly show that there is a relative rotation between the third and fourth sections of shaft.

Diagram I-18 - the obviously rotated middle section of shaft

On the image, the angle of the top of the doorway is not caused by the right corner of this bend being set further down the shaft as may first appear, but is caused by the camera being rotated, which can be seen clearly when Sibson's image 25 is rotated so that the fourth section of the shaft is rectified in diagram I-19.

Diagram I-19 - The rotation apparent at the top of the third section of shaft.

Evident in this image is that the longitudinal axis rotation of about 12^{o} and a bend to the right in the shaft (ascending) of about 18^{o}. The longitudinal axis rotation is not an absolute value but is a relative rotation between the second and third sections of shaft, and therefore does not help in providing the absolute rotation of the the second shaft section but does show that all the sections of the shaft are each rotated around their longitudinal axis.

To determine an angle of rotation of the second shaft section, it is necessary to look at the debris fields in many of Sibson's other photographs. Diagram I-20 shows the most relevant of these images with their original framing, and their rotated framing in which the debris field is lying with its top in a horizontal position - there have been several Earthquakes in Egypt since the late 1800s, with the large one on October 12, 1992 in the Cairo region on its own sufficient to shake these debris piles horizontal.

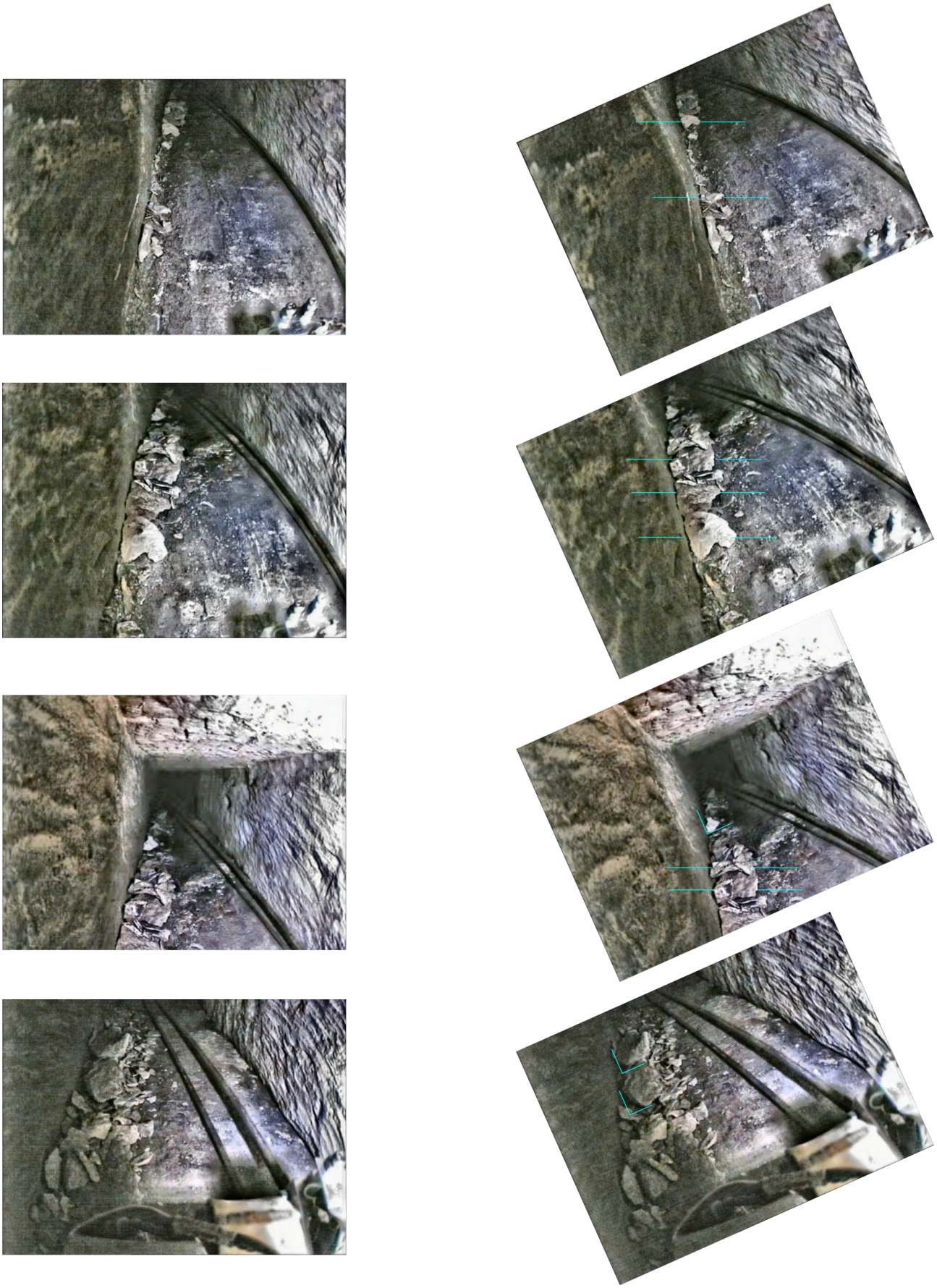

Diagram I-20 - The debris fields in the second section of the shaft.

The estimation of the angle of rotation of the Pyramid Rover robot's camera relative to the horizontal on each of these images was determined by looking for marker stones in the debris that show signs of being horizontal, and which are marked on each rotated image with the pairs of horizontal lines. The stones marked with two lines at right angles show signs of being at rest in the lower left corner of the shaft.

From this analysis the average longitudinal angle of rotation of the second section of shaft is 24 degrees, which is the same as the second angle that was shown in the shaft rotation diagram I-11. The z-axis rotation of the shaft and the longitudinal axis rotation of the shaft add up to 90 degrees, and therefore both are given to us by the architects in the design of the bend point between the first and second sections of shaft.

It is now possible to rotate section two of the shaft around its U axis on the 3D model, cut the floor of the lower section of the shaft along the line of the square metal rod, slice the floor section of the second section of the shaft along the same line, and look at the resulting photo taken inside the model, which is shown in illustration I-21.

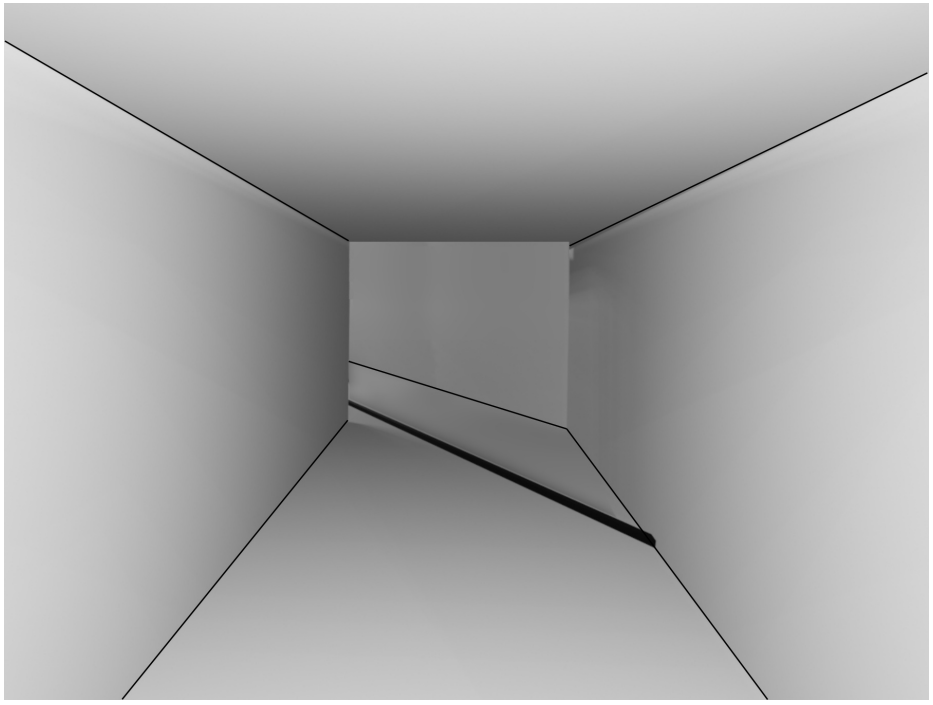

Diagram I-21 - A rendering of a 3D model of the corner of the shaft after angle 'bisection' modelling.

Sibson's door

With the longitudinal axis rotation of the second section of shaft being set at 24^{o} there is a problem now with the shaft side hole and the stone ball. In diagram I-5 the ball was shown at rest in the side door of the shaft, but with the shaft rotated on its U axis, this stone ball would immediately roll out into the shaft and descend down to the lower chamber of the pyramid. And because this is the only location that the ball could have been situated in, then the conclusion must be that *the door was originally shut* and the ball was positioned behind the door, and that when Waynman Dixon started to poke inside the shaft in 1872 he triggered the door to open.

To understand how this was achieved by the architects another visit to Gantenbrink's door is required. When the door was drilled through by the Djedi robotics team, they inserted a small camera through the hole and observed the back of the door, discovering the rear side of the metal 'seals' that are evident on the front of the door. Diagram I-22 is a reproduction of the image from the Djedi team's project report showing the front and back of Gantenbrink's door, with the dimensions of the door's height and the hooks diameter added.

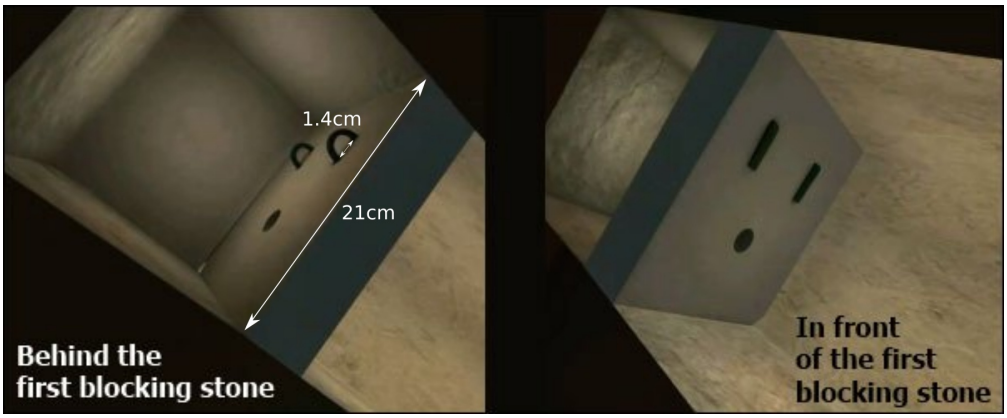

Diagram I-22 - The diagram from the Djedi project report, with dimensions added.

What is of interest is the two semi-circular metal pieces on the back of the door, which have an internal diameter of about 1.4cm on the illustration created by the Djedi team. It was shown earlier in diagram I-4 that the side hole in the second section of the lower northern shaft perfectly matches the shape of the front of the metal seals on Gantenbrink's door, but that the door would need to be inverted for this match to occur. The door also needs to be inverted back to front in the architect's design system, so that the two semi-circular metal anchor points that are on the back of Gantenbrink's door are located inside the second section of the lower northern shaft on the missing door panel that would fit into the side hole of the shaft.

Diagram I-23 shows the door construction as it was before being sheared off when Waynman Dixon interfered with the contents of the lower northern shaft. The second section of shaft is rotated by 24^{o} around its longitudinal axis, the part of the side door that detaches from the wall is shown in a grey colour to distinguish it from the right side wall of the shaft, and the ball is shown in x-ray style behind the door. (The area behind the side door is shown running perpendicular to the right side wall, and this is for illustrative purposes only as the angle at which it comes off the shaft side is unknown.)

On the near side of the shaft floor is the 5mm x 5mm cross section metal rod, that is shown in Sibson's image number 21 in this approximate position. Because the origin of this rod has already been shown to be an original part of the pyramid's architecture, then it can be seen in diagram I-23 that if the metal rod acted as a spring and was placed under tension on the opposite side of the shaft to where it now resides, and threaded through the two anchoring rings on the door, a mechanism for removing the door would be created that would be triggered by anyone exploring the shaft below this point.

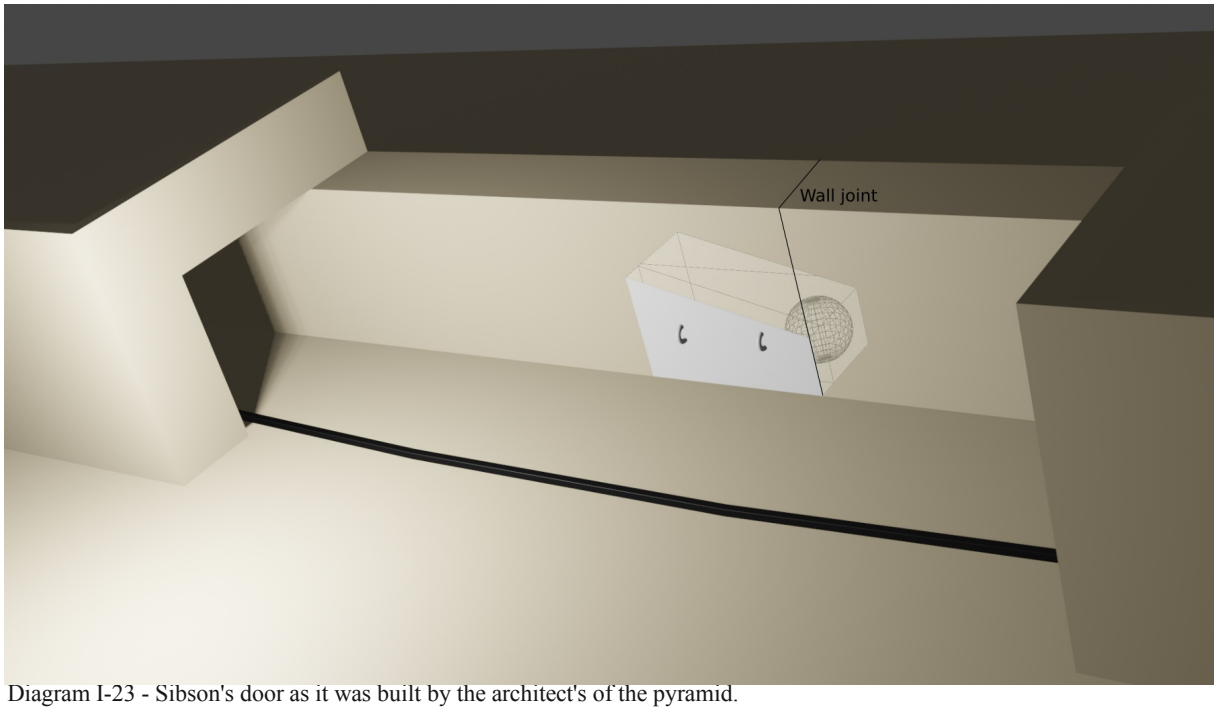

Diagram I-23 - Sibson's door as it was built by the architect's of the pyramid.

For such a spring mechanism to work, it would need to be loaded under tension, and for that to be possible the end locations of the metal rod would need to allow the tension to be placed in the rod, and so the rest of the shaft's construction needs analysing. Diagram I-24 shows image numbers 22 and 23 from Sibson's collection in which the distinct bend to the right between shaft sections two and three occurs.

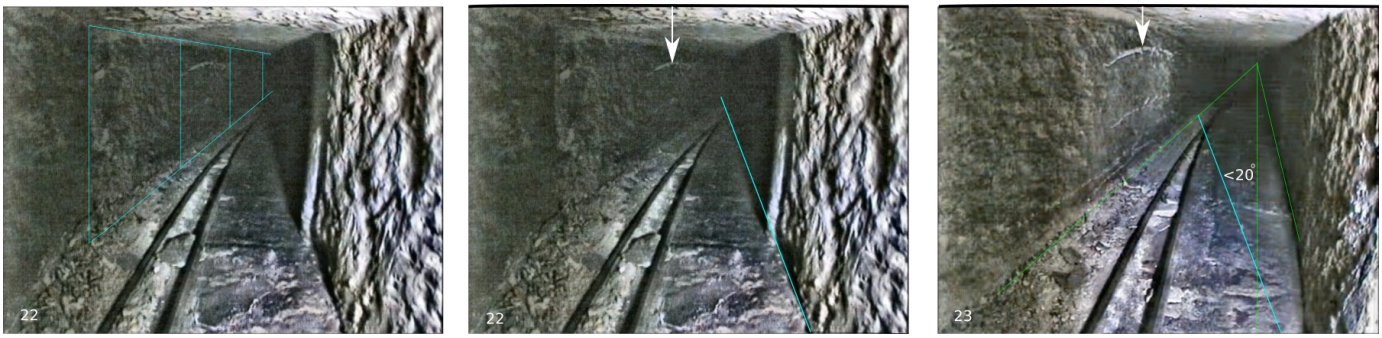

Diagram I-24 - The small bend in the shaft after the doorway in section 2.

The left image of the three shows the left wall length, estimated by forming 21cm squares along it, from which the shadow from the right wall can be seen to intersect the left wall at a distance of 3 squares, making the bend in the shaft, by trigonometry, atan(1/3) or 18.4°. The second image shows the position of a wall marking with the white arrow, which appears in exactly the same position across the photo width in the third image, meaning that the robot must have moved up the shaft parallel to the shaft section's central axis between Sibson's images 22 and 23 and therefore the vanishing point lines must be consistent across the two images. The third image has the lower right vanishing line from image two superimposed upon it, and the angle between the right sidewall of the shaft around the bend and the line can be measured at 20°, meaning the angle on the floor will be just less than less than this at around 18°.

These angular measurements and the lengths of each shaft section can be checked and a full 3D construction of the shaft can be undertaken by referring to the article written by Zahi Hawass[5] for the 43rd edition of the Supplément aux Annales du Service des antiquités de l'Egypte, in which he publishes much of the basic principal length data from the Pyramid Rover exploration, which can be cross checked against SCA final report[6] regarding the exploration.

Because it was determined earlier that the longitudinal rotation angle between the third and fourth sections of shaft was about 12 degrees, the outline of the system that the architects have used for the full shaft can be seen. Giving the axis rotations the convention letters that are used in 3D systems, where the reference frame has X,Y and Z axis and the object being rotated has the same axis labeled U,V, and W then

		X	Y	Z	Bend	U	V	Z
A	Horizontal shaft section	0	0	0	0	0	0	0
B	First section of shaft	40	0	0	0	0	1.6	0
C	Second section of shaft	40	0	66	66° left	0	24	0
D	Third section of shaft	40	0	48	18° right	0	12	0
E	Fourth section of shaft	40	0	30	18° right	0	0	0
E	Fifth section of shaft	40	0	45	15° left	0	0	0

Table 1 - The approximate interpolated rotation angles of the shaft sections

The fifth section of the shaft data has been interpolated from the known sections of shaft with the 45° z-axis rotation angle being based on the logic in the other shafts of the building.

Diagram I-25 shows the completed 3D model of the lower northern shaft in plan view, the orthogonal projection plane being parallel to the average floor plane of the shaft and the shaft sections being joined along the west wall of the shaft at the joints.

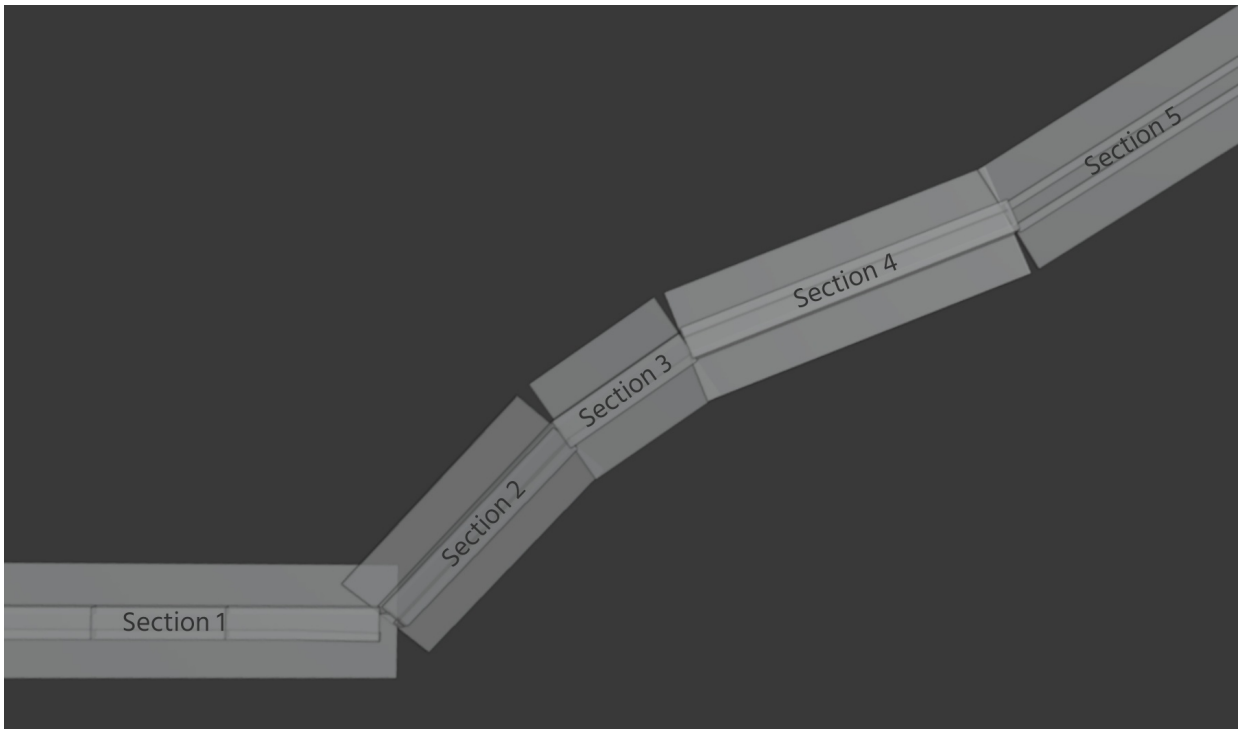

Diagram I-25 - The lower northern shaft bend positions and angles.

Diagram I-26 shows the tradition orthogonal projection of the pyramid taken from the East, on which it can be seen that the bend points in the shaft are aligned with the overlaps on the gallery walls, by design.

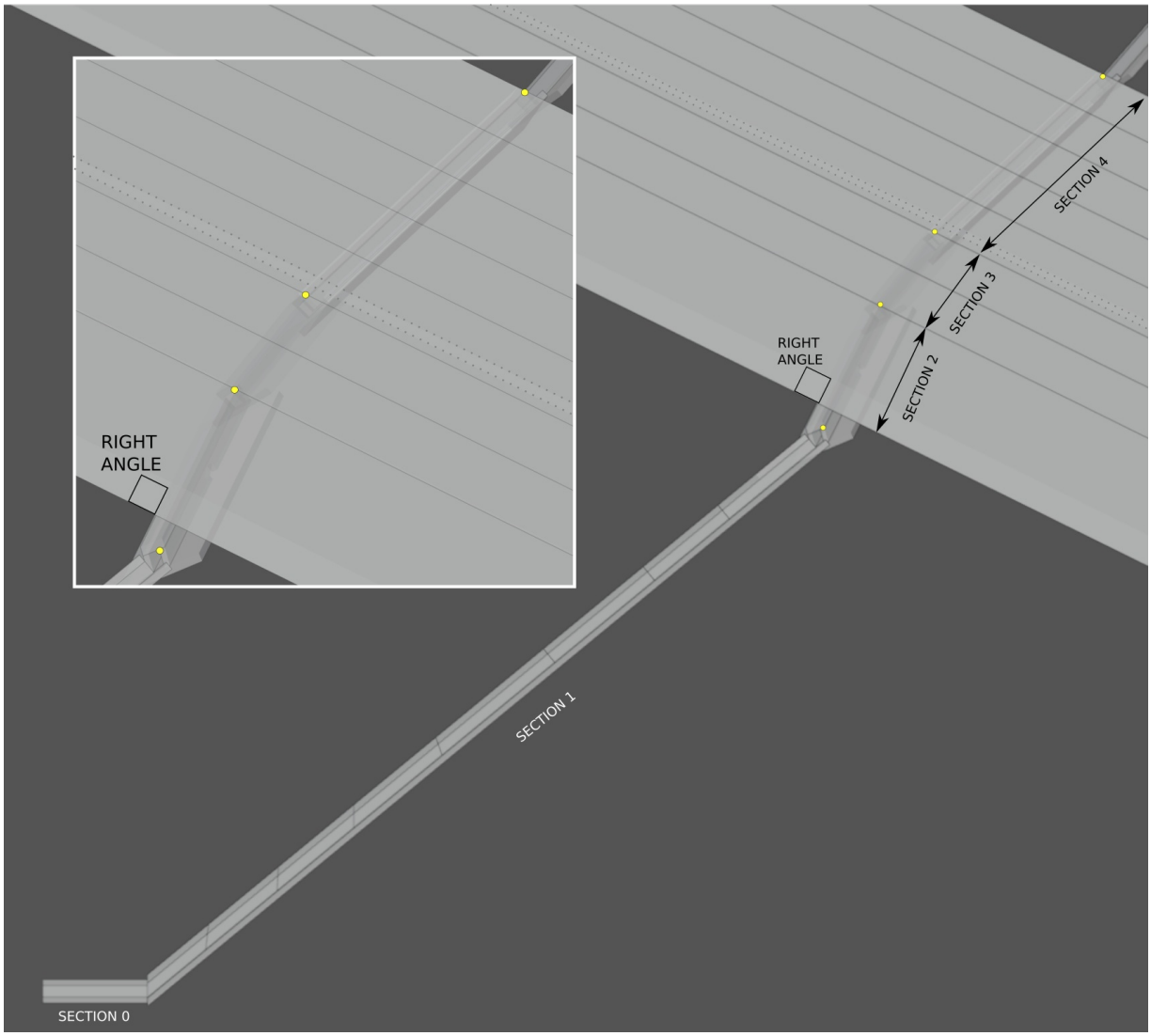

Diagram I-26 - Classic orthographic projection from the East, showing the lower northern shaft and the gallery.

The architects and builders of the pyramid knew exactly what they were doing with this complex three dimensional geometry, and the coordinates of the bend points in the shafts can be calculated accurately from the shaft's bend angles when aligned with the measurements of the heights of the gallery walls.

Within the Pyramid Rover report and that of Zahi Hawass there is no mention at all of the small side opening in the second section of shaft, Sibson's door. Luckily the Pyramid Rover photographs are continuous from the bend between sections one and two, as shown in the photograph analysis of diagram I-27, from which the position of the right side of Sibson's door can be determined as being half way along this shaft section.

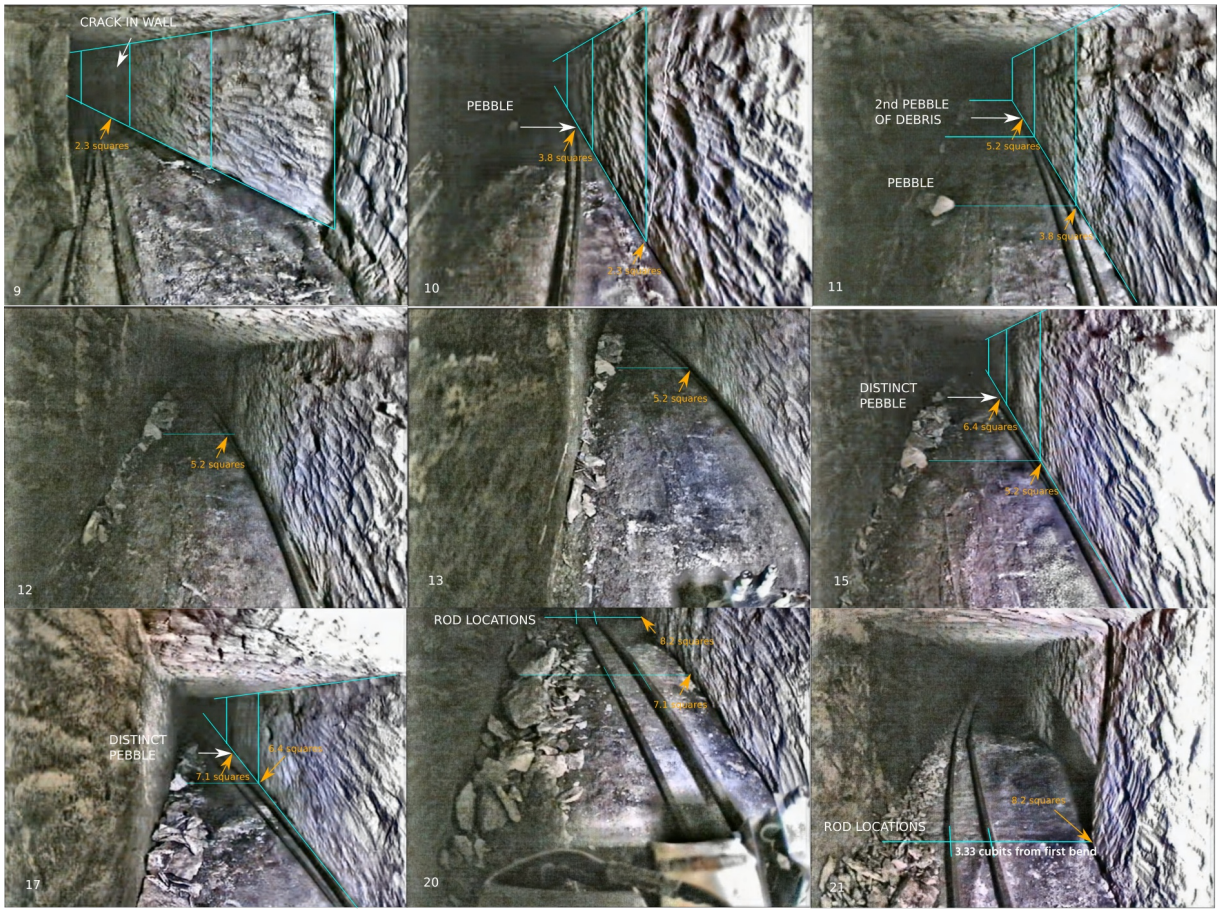

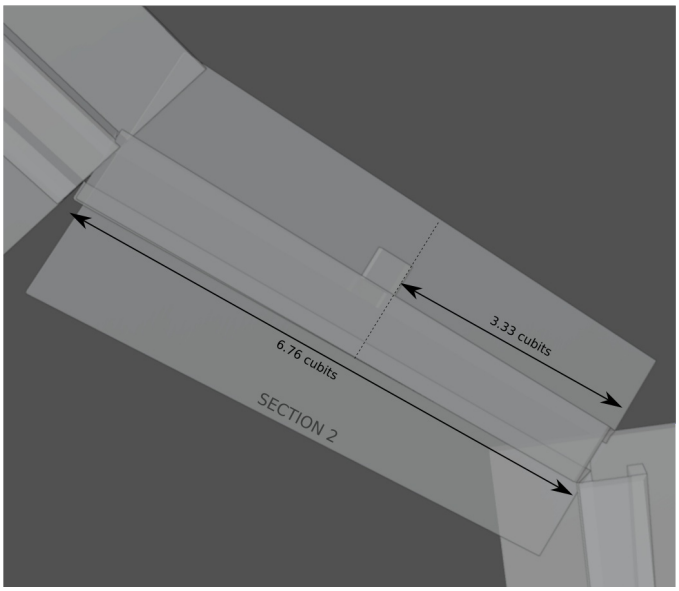

Diagram I-27 - The photographic analysis of the position of Sibson's door.

With all of the component parts of the shaft now analysed to the point where the location of the bends is known, it is possible to model the square rod in the shaft and show the position it was found in when first seen by the Upuaut robot, and then the position in would take if threaded through the hooks on the front of the side door of section two.

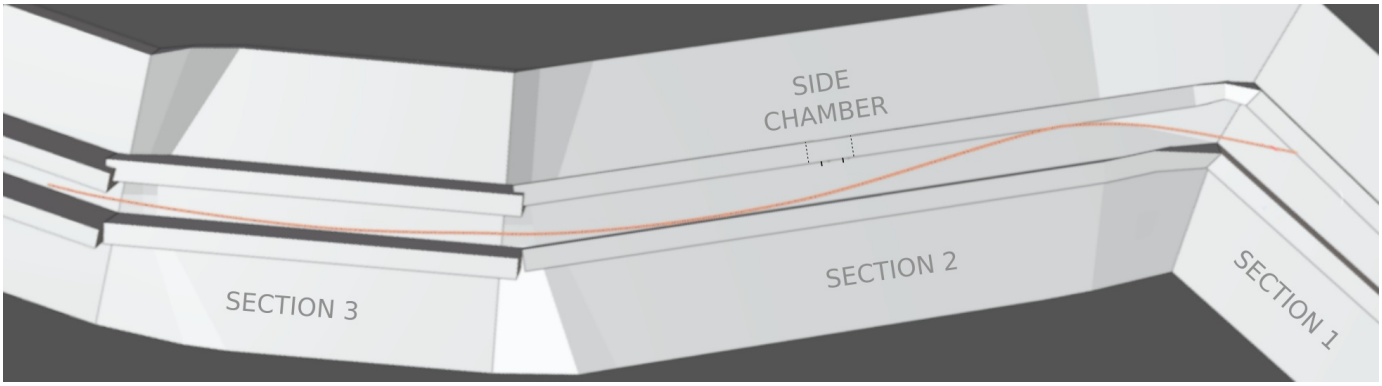

Diagram I-28 - The square rod at rest in the lower northern shaft, 1997 position.

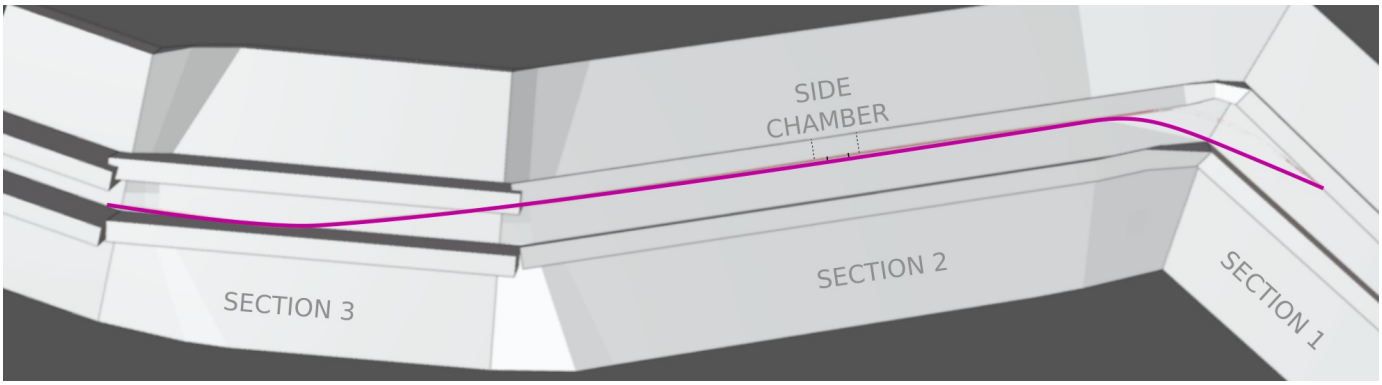

Diagram I-29 - The square rod used as a spring under tension, as built at the time of the pyramid's construction.

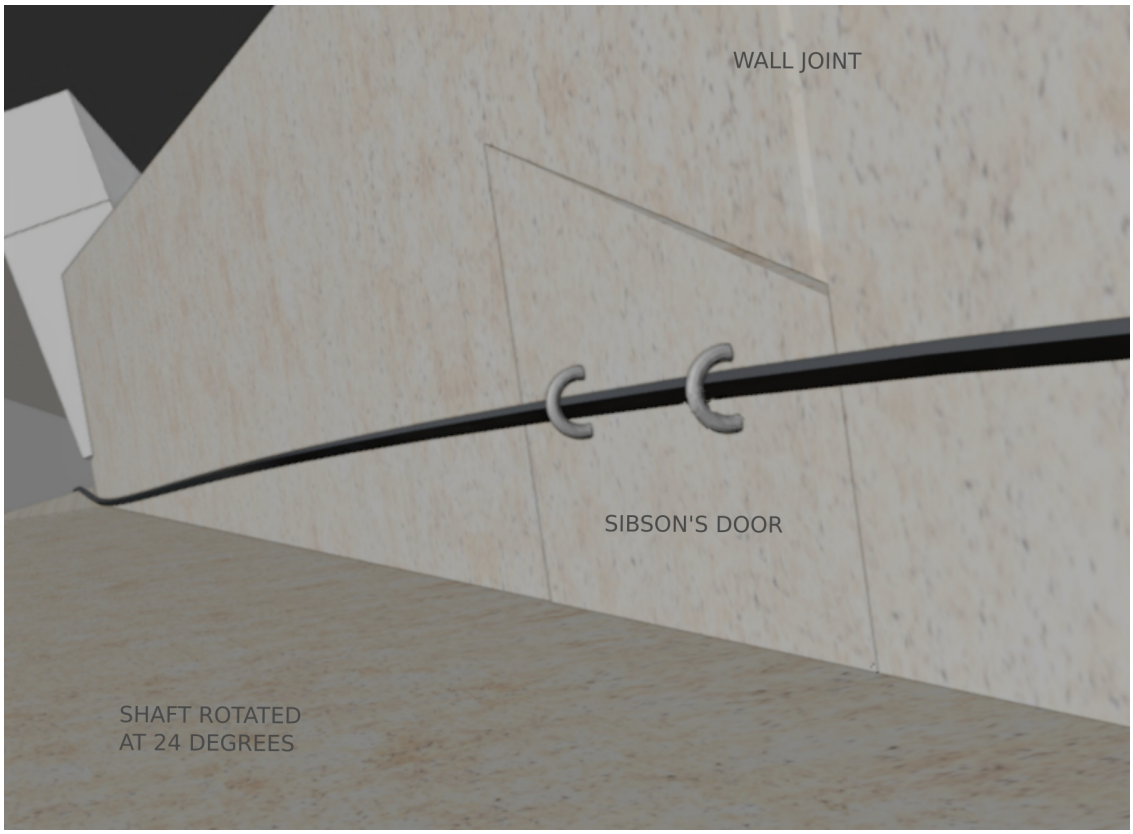

Diagram I-30 - A close up of the front of Sibson's door with the sprung metal rod running through the metal door loops.

The trigger mechanism

Diagram I-29 shows the square rod spring under tension, and if one considers the mechanics of this system where the top of the rod is responsible for providing the tension in the system by being forced against the left (ascending) wall of the shaft, then the bottom end of the rod would slide down section one of the shaft when the spring was put into place.

During Gantenbrink's robotics exploration of the shaft he noted an unusual hinge shaped piece of metal which was located underneath the hexagonal rod at this rod's first bend point close to the easterly right wall of the shaft. Gantenbrink's image is shown in diagram I-31 alongside a 3D model close up of the same.

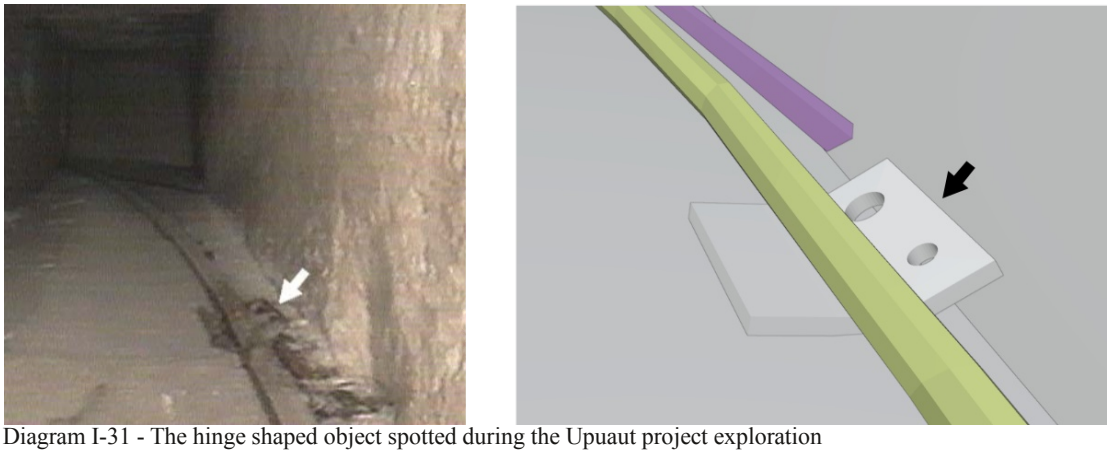

Diagram I-31 - The hinge shaped object spotted during the Upuaut project exploration

Looking at the sprung metal rod system, it is most probable that the lower end of the square rod was attached to the piece of wood and the metal hook that were mentioned on page 2 as having been found inside the lower northern shaft when it was first explored. A logical mock up of how these items were attached together taken from the 3D model is shown in diagram I-32, where the lower end of the square rod is attached to the piece of wood which is split like a peg at the end, and the hook slid into it. Because this end of the system is not under tension, it sits on top of the hinge shaped object and is not connected to it.

When any pressure is applied to the trigger hook, the force is transferred through to the metal rod spring and the slight increase in tension inside the rod causes it to snap into its unloaded natural shape. Sibson's door is known to be located at a wall joint, so the right side of it would not have been attached to anything, and if the diagonal line of the top of the door and the left edge were etched deeply into the door, then the increase in tension on the door hooks would cause the door to detach from the wall. There is evidence in the photographs that this is the case because the left side of the door jamb is rounded off, suggesting it has undergone a trauma, and there are scrape marks across the shaft where an object has slid from right to left in front of the side chamber as shown in diagram I-33.

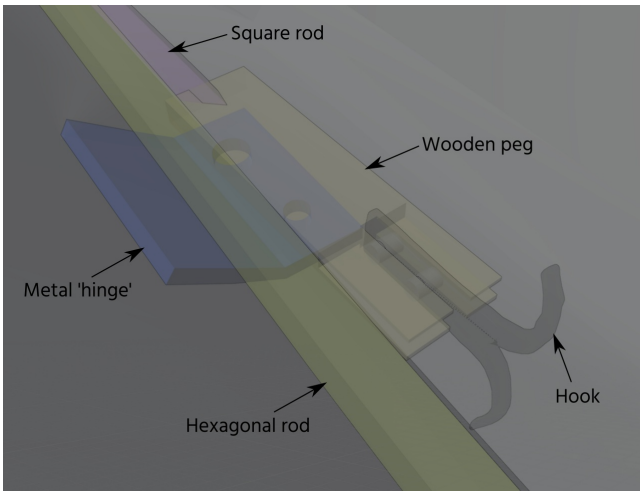

Diagram I-32 - The trigger mechanism

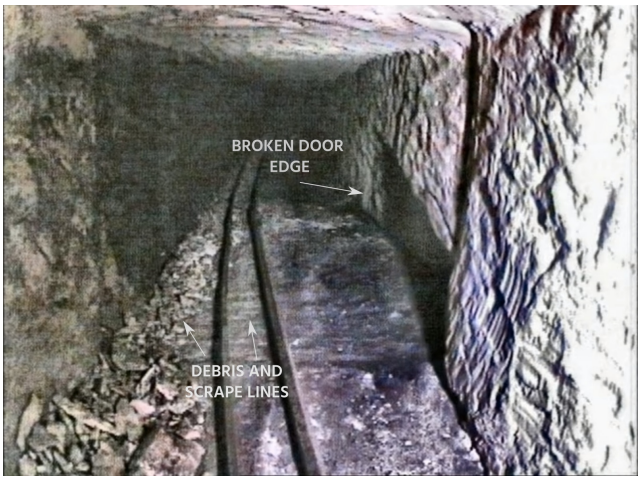

Diagram I-33 - The evidence of the door detaching from the wall

As soon as the door detached from the side wall and had moved just 1mm on its journey towards its inevitable destruction on the other side wall of the shaft where it would smash into small pieces creating the debris piles currently seen in the shaft, the majority of the tension would still be in the sprung rod. This would cause the lower end of the metal rod to move rapidly up the shaft and the hook would catch on the hinge shaped object, detach from the wooden peg, and then drop down the shaft. The detached lower end of the spring with the peg still attached would smash against the right side wall of the shaft, causing the wooden section to detach from the metal rod and also start its descent down the shaft.

The final part of this mechanical system would be that the stone ball would roll out of the side chamber of the shaft, because of the longitudinal rotation angle of the shaft, and then follow the path of the rod as it descended down the shaft to appear before whoever set off the trigger mechanism.

The purpose of the lower northern shaft

As with all of the other parts of the Great Pyramid, there is a mathematical purpose behind the wonderfully creative architecture on display. The lower northern shaft was made particularly difficult to gain access to and contains sufficient artifacts and an ingenious mechanical spring mechanism that cleverly self-disguises once triggered, to make it quite obvious that it is among the most important parts of the building's design. The mathematical data contained in the shaft is impossible to calculate without knowing what lies around the bend in the lower northern shaft, by design.

During previous research[7] I determined that the lower northern shaft's orthographic projection, the classic east view of the pyramid, contained a dynamic piece of geometry formed from a one fifth sized model (in comparison to the main model identified in the previous paper[8]) of the Earth on which the axial tilt of the planet oscillates between +23.5 degrees and -23.5 degrees. The animation of this can be seen on the referenced webpage, and the position, angle and length of the upper and lower sections of the shaft can be explained using this system which was reverse engineered from knowing the headline information from the Pyramid Rover exploration that was released to the public some years ago.

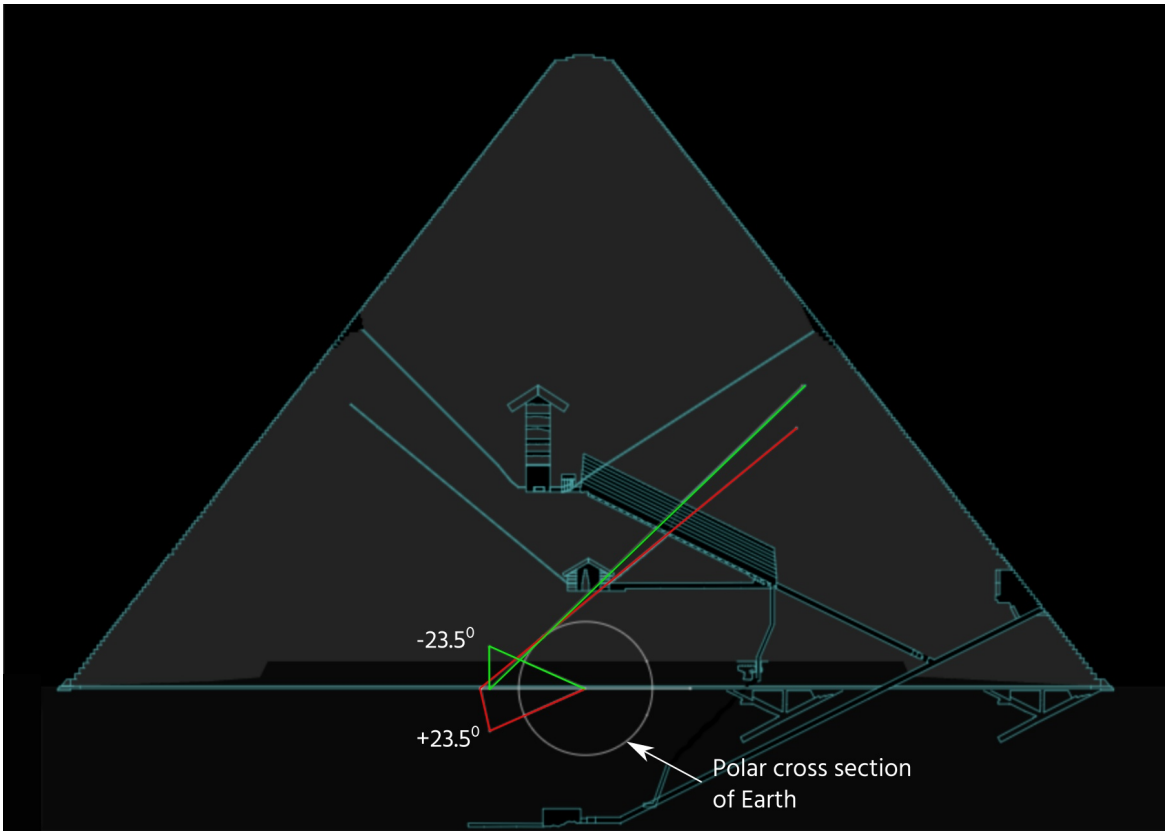

Diagram I-34 - The dynamic geometry of the lower northern shaft

This geometry, when looked at in association with the analysis of the lower northern shaft in this paper, produces a self regulating piece of iterative mathematics which works as follows:

1) Create a two dimensional polar cross section ellipse model of the Earth using the ellipsoid data from the upper chamber that was discovered in the last paper in this series but at one fifth scale, and place it centrally at ground level within the pyramid, with no axial tilt applied to it.

2) Calculate the tangent line to the ellipse (the red line on diagram I-34), drawn from the half circumference point at ground level, resulting in a tangent line angle of 39.5252^{o}.

3) Apply this as the elevation angle of section one of the shaft and then calculate the rotation angle of the second section of the shaft around the vertical axis that is required to make its easterly orthographic projection perpendicular to the gallery floor, giving a result of 63.72^{o}.

4) Calculate the longitudinal-axis rotation angle of the second section of shaft by deducting the value in 3. from 90^{o}, to give a second shaft section rotation of $26.2814^{o.}$

5) Plug this value back in as the axial tilt of the Earth model and then go back to step 2 and continually repeat the calculations until the axial tilt value stabilises.

The following list shows the values of each run of the geometry and associated numerical output.

Earth Axial Tilt	Shaft section 1(Y axis)	Shaft section 2 (Z-axis)	Shaft section 2(U axis)
0	39.53	65.96	24.04
24.04	39.472	66.0039	23.9960
23.9960	39.472127	66.003931	23.996068
23.996068	39.472127116	66.003931151	23.996068848
23.996068848	39.472127116841	66.003931151013	23.996068848986
23.996068848986	39.47212711684154	66.00393115101389	23.996068848986106

Allowing us to obtain this value of the axial tilt of the Earth is the primary purpose of the lower northern shaft's engineering design. The precise angular value that is obtained allows the 'date of the pyramid' to be obtained. The Great Pyramid is a monument and contains not just a model of the Earth, but an astronomical model of the Earth at a particular moment in time, and it is this moment in time that can be extracted from the rotation angle by using Laskar's axial tilt formula[9] in reverse. If an estimated date of 4000 BCE is used as a starting guess for the pyramid's date, and then the formula is run iteratively until the axial tilt angle obtained stabilises to that extracted from the lower northern shaft geometry, then the 'T' value in Laskar's formula is -0.4727927850691. The unit of this variable is important as it is 10,000 Julian years referenced to the J2000 epoch, and so it is necessary to calculate the Julian date of the moment in time, giving JD 724669.352535113, and then convert this into commonly used date and time formats. The result is **BCE January 14th 2729 20:27:39**.

This value can be checked as being realistic or not by using NASA's DE441 ephemeris and checking to see if there is a solstice close to this date and time. (The reason the event must be a solstice is that the principal axis of the pyramid's passages runs north to south, and therefore if the axial tilt is applied from the east, this will produce a solstice event along the north south axis.) The result from NASA's ephemeris is that the northern hemisphere's winter solstice occurred on **BCE January 14th 2729 17:29:26** at JD 724669.228769627, showing a discrepancy to the date and time just obtained from the lower northern shaft of just 3 hours. Laskar's formula is intended as being a close approximation formula, so no further analysis of the difference between these two times of the event is of any significance.

The following diagram I-35 shows the data extracted from the DE-441 ephemeris for all of the major orbital events of the Earth around the year 2729 BCE starting at the perihelion event at the end of year 2730 BCE and ending at the winter solstice at the start of January of the year 2728 BCE, with the normalisation number showing the event date as a proportion of a 365.25 day Julian year from the base value of 0 at the event just determined from the axial tilt, the winter solstice 2729 BCE.

EVENT	NASA JPL DE-441	
Perihelion	BCE 2730-Nov-05 13:07:23.553 JDUT 724599.046800380 JDTDB 724599.796835039 Normalised (TDB) : -0.1921473944	Mean anomaly : 0 deg True anomaly : 0 deg Eccentricity : 0.01918124702358505 Semi major axis : 149721917.76894 km
Winter solstice	BCE 2729-Jan-14 17:29:26 JDUT 724669.228768998 JDTDB 724669.97867086 Normalised (TDB) : 0	Mean anomaly : 69.38065089707172 deg True anomaly : 71.32232872667144 deg Eccentricity : 0.01796439316977578 Semi major axis : 149542773.93497 km
Spring equinox	BCE 2729-Apr-12 21:14:23.447 JDUT 724758.384993597 JDTDB 724759.146426382 Normalised (TDB) : 0.244128009642893	Mean anomaly : 157.9908579967649 deg True anomaly : 158.7759573478909 deg Eccentricity : 0.01867872326630539 Semi major axis : 149535049.62156 km
Aphelion	BCE 2729-May-05 19:31:21.947 JDUT 724781.313448466 JDTDB 724782.074869107 Normalised (TDB) : 0.306902664605194	Mean anomaly : 180.0142190621463 deg True anomaly : 180.0137242910761 deg Eccentricity : 0.01778528365468130 Semi major axis : 149693762.32456 km
Summer solstice	BCE 2729-Jul-19 09:26:11.858 JDUT 724855.893192799 JDTDB 724856.654472475 Normalised (TDB) : 0.511090490390457	Mean anomaly : 250.8188051783684 deg True anomaly : 248.8542867163617 deg Eccentricity : 0.01829131993749967 Semi major axis : 149515008.90376 km
Autumn equinox	BCE 2729-Oct-14 03:37:11.435 JDUT 724942.650826799 JDTDB 724943.41189593 Normalised (TDB) : 0.748619370485996	Mean anomaly : 337.9258189155223 deg True anomaly : 337.1515891880403 deg Eccentricity : 0.01761251925135706 Semi major axis : 149477231.26586 km
Perihelion	BCE 2729-Nov-06 03:46:12.953 JDUT 724965.657094366 JDTDB 724966.40679649 Normalised (TDB) : 0.811575977084234	Mean anomaly : 0 deg True anomaly : 0 deg Eccentricity : 0.01784274254047189 Semi major axis : 149511391.43048 km
Winter solstice	BC 2728-Jan-13 23:28:40.474 JDUT 725034.478246231 JDTDB 725035.227816407 Normalised (TDB) : 0.999997660635303	Mean anomaly : 70.18817254514830 deg True anomaly : 72.20442917654034 deg Eccentricity : 0.01855895170818702 Semi major axis : 149538002.96510 km

YEAR LENGTH

JDTDB 365.249145547

JDUT 365.249477233

Diagram I-35 - The data from the NASA DE441 ephemeris for the year 2728 BCE

What can now be done is to match up this table of information to the architecture within the pyramid. If the architect's system is followed methodically the only event known at this stage is the winter solstice 2729 BCE, so a model of the Earth at this solstice position directly in front of the entrance to the lower northern shaft, along with the earth's tangent line, can be added to the 3D model of the pyramid. Diagram I-36 shows these elements correctly positioned in 3D within the pyramid's structure, with the tangent line to the Earth running up section one of the lower northern shaft.

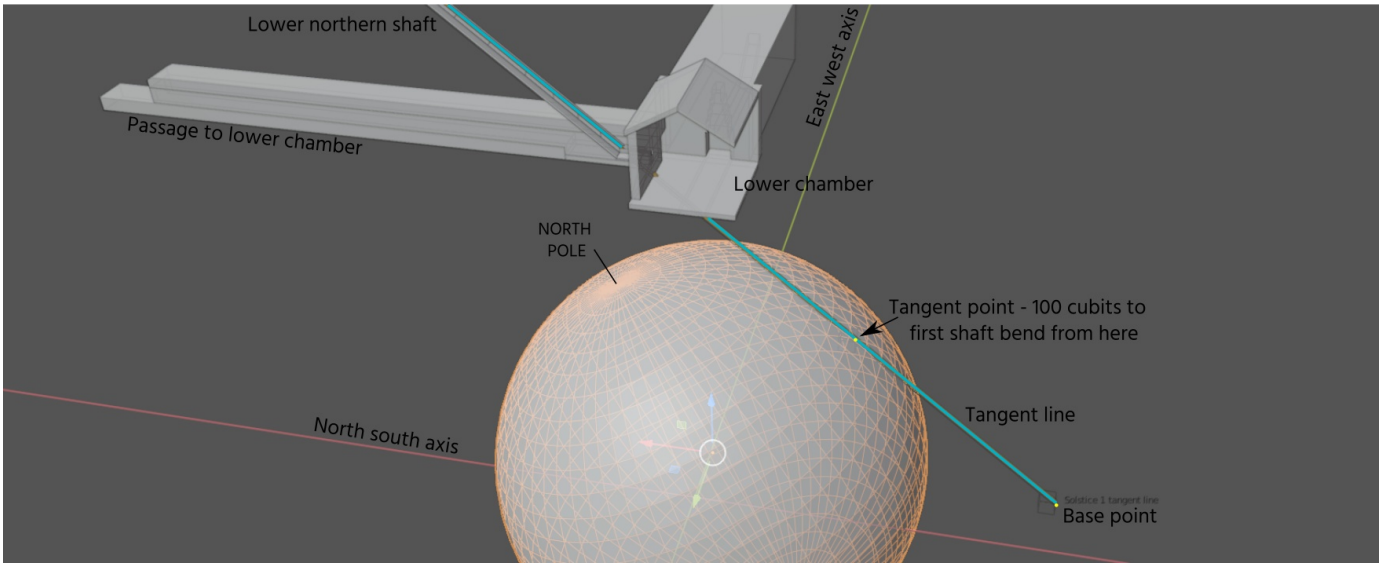

Diagram I-36 - The geometric elements from which the first section of the lower northern shaft is formed.

In order to obtain more information about the other events during the year, there must be a system in place within the architecture that allows the Earth model to move along the east-west axis line, and so more analysis of the building's architecture is required. On the lower chamber's east wall there is a large carved structure known as the 'Niche' and whilst it is in itself a fascinating feature of the building, what is of interest is the roughly cut tunnel that starts at the back of the Niche and makes its way into the core masonry towards the east side of the building. The dimensions of this tunnel are shown in the work of Maragioglio and Rinaldi[10] giving the length of the tunnel as 15.30m.

If this tunnel length is compared to known values from the earth model it can be deduced that the end of the tunnel is located one quarter of the polar circumference of the Earth model away from the north south central axis of the building, *c*/4. Additionally, the position of the start of the lower northern shaft can be determined from the architects measurements because the north east corner of the chamber wall is known to be 15 cubits from the central axis from the work in a previous paper[11], and from surveying measurements the west side of the shaft is exactly 3 perfect meters from this point.

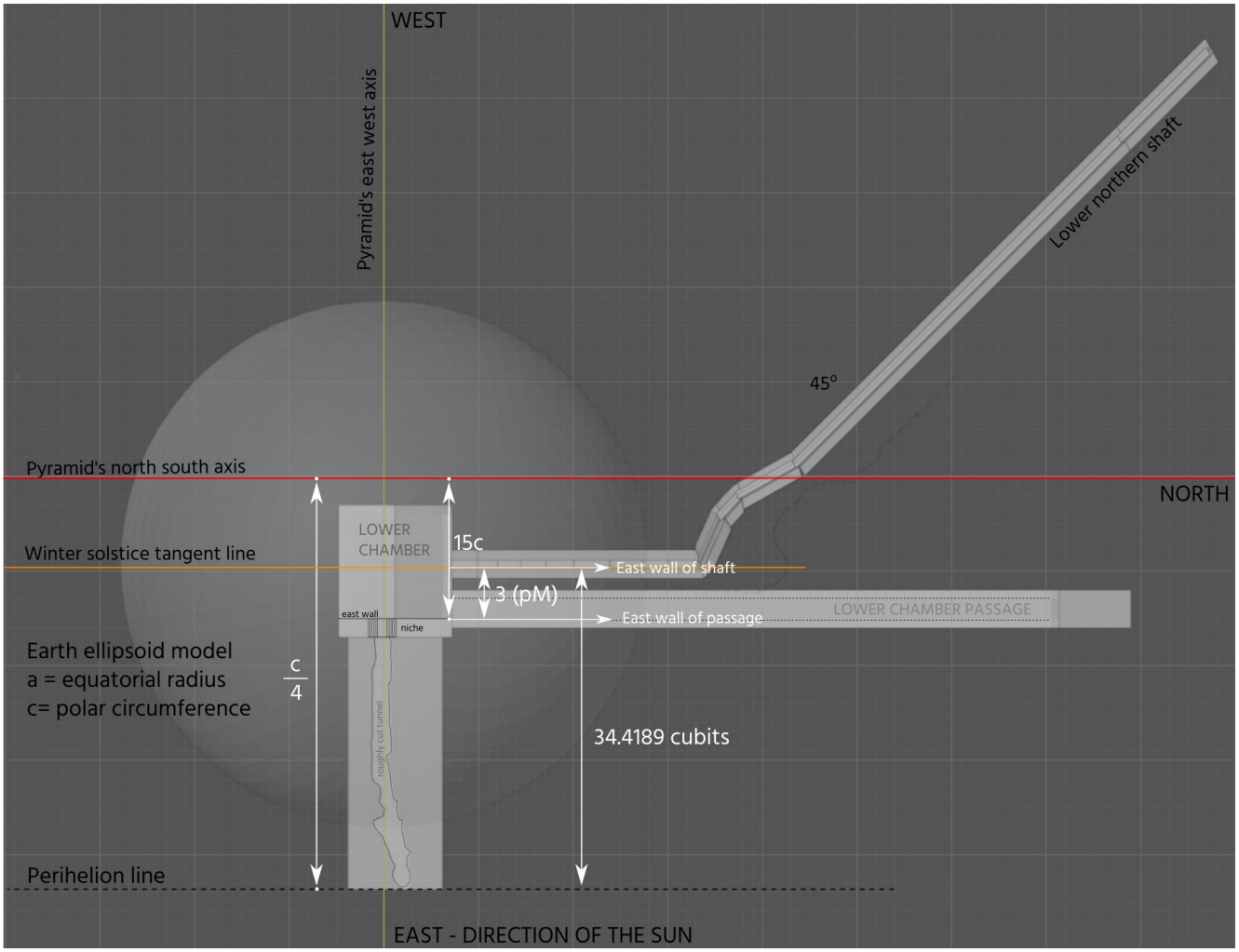

Diagram I-37 - The distances from the central north south axis within the architecture.

Analysis of the data in comparison to the DE441 data shows that the east end of the tunnel is the orbit's perihelion point, and the west wall of the shaft is a winter solstice point. Working out the distance that are shown in diagram I-37 yields perihelion at *c*/4 =43.6853 cubits east of the central axis and winter solstice at 15c -3pM =9.2663 cubits east of the central axis and therefore the distance between these two events is 34.4189 cubits. *Using the 2728 BCE winter solstice and the 2729 BCE perihelion* from the DE441 ephemeris data in diagram I-35, the JDUT time difference between these two events is 18.8422% of a Julian year, from which the distance in the pyramid for the full year length can be calculated proportionally as 365.34 / 2 cubits. It can be seen that the architects have designed the orbit's unit system to be recognisable so that a nominal average year, 365.25 Julian days, of movement of the Earth around its orbit

is represented by half this number of cubits of movement along an east-west direction in the building. What is more, by tying in a recognisable time value into this definition it allows the two locations that appear on the east-west track line to be identified as mean anomaly time values, as opposed to true anomaly angular values, which they also could have been.

Because the length of the track line is now established as being 365.25 / 4 cubits, and the mathematical location of the end of the tunnel and the shaft wall are known, a comparison of the pure pyramid data can now be made with the DE441 ephemeris data. In the pyramid, the time span between perihelion and winter solstice can be calculated from the cubit distance between the locations as a proportion of the track length, giving exactly 18.8467847 % of a year, and in the DE-441 for JDUT it is 18.84220448 %. The difference between these values is 0.00458% of a year, or 24 minutes and 5.4073 seconds of time, with the error most likely in the modern data. Within the DE441 ephemeris, at dates 4500 years ago, their error margin is specified as between 18 and 36 minutes for events along track. From private correspondence :

"[Errors are] 350 km uncertainty in along-track position by 2500 BC, growing to 366 km by 2600 BC. With geocentric velocity of ~ 0.97 km/s at apoapsis, this implies 340-355 seconds of uncertainty in apoapsis time. These results were obtained by differencing ephemeris solutions LE422L - LE406. LE422L is a recent experimental solution that includes another 15 years of tracking data, LE406 is the current standard Horizons uses. The difference between the solutions is a useful guide to real error levels, but multiplying values by ~3-6 to allow for uncalibrated error sources common to both isn't unreasonable."

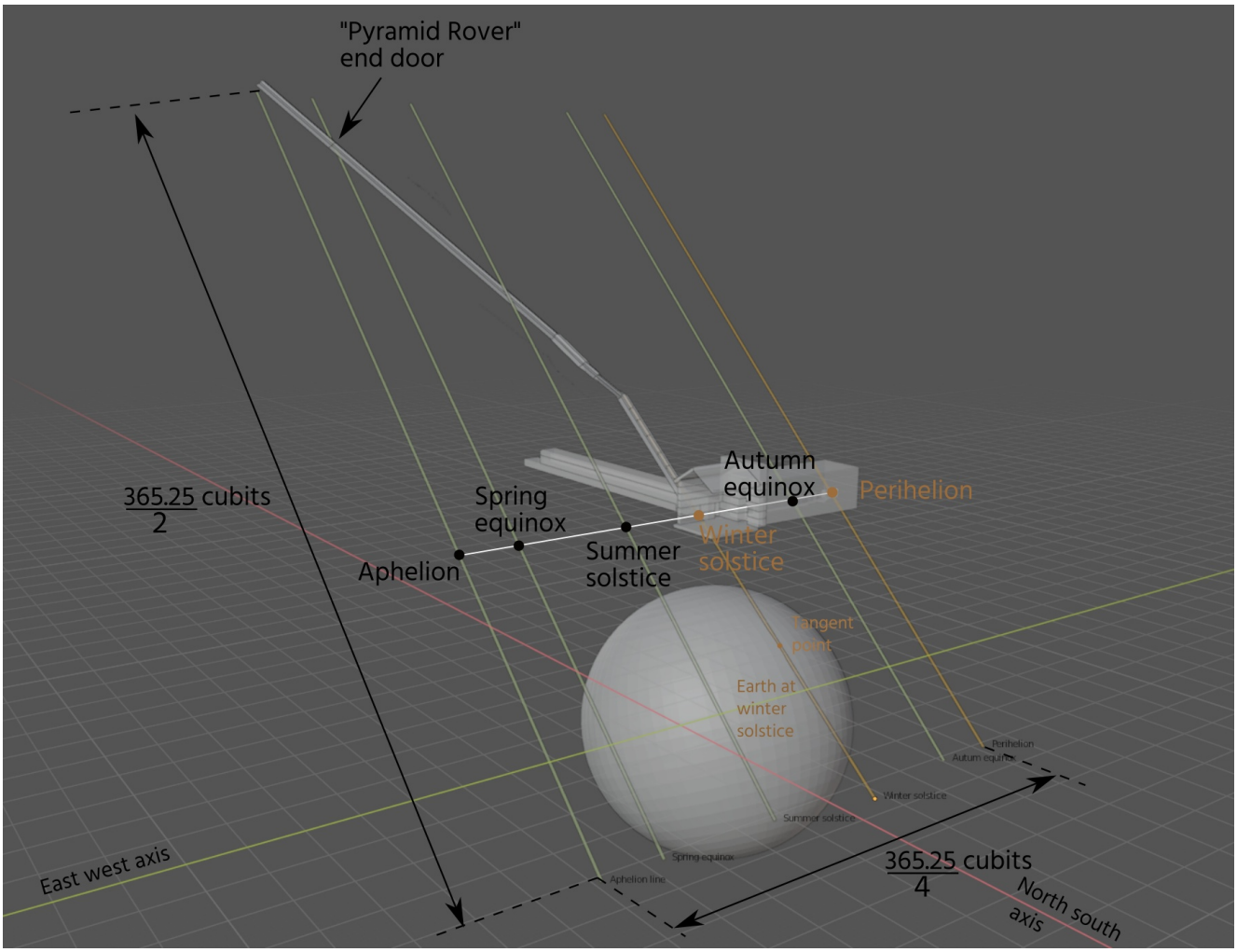

Diagram I-38 - The annual astronomy events from NASA's DE441 marked along the Great Pyramid's east-west axis.

Having revealed this part of the architectural system it is now possible to go back to the 3D modeling software and mark off the points along the east west axis that correspond to the astronomy events that were listed in the DE441 output and match them up to features within the pyramid, as shown in diagram I-38. In this diagram the events are marked off using tangent lines to the Earth as it moves along the track line of

its orbit, but with only one earth model shown at the position of the winter solstice. The two tangent lines drawn in orange are the two points that are explicitly defined with absolute numerical precision in the architecture. The green lines are taken from the DE441 ephemeris and correspond to the points in the pyramid shown in the diagram. The end door that was discovered by the Pyramid Rover team is built at the y coordinate that matches the spring equinox of 2729 BCE. The section behind the door at the top of the shaft is modeled using the aphelion point on the orbit, and this tangent line has a length of 365.25/2 cubits.

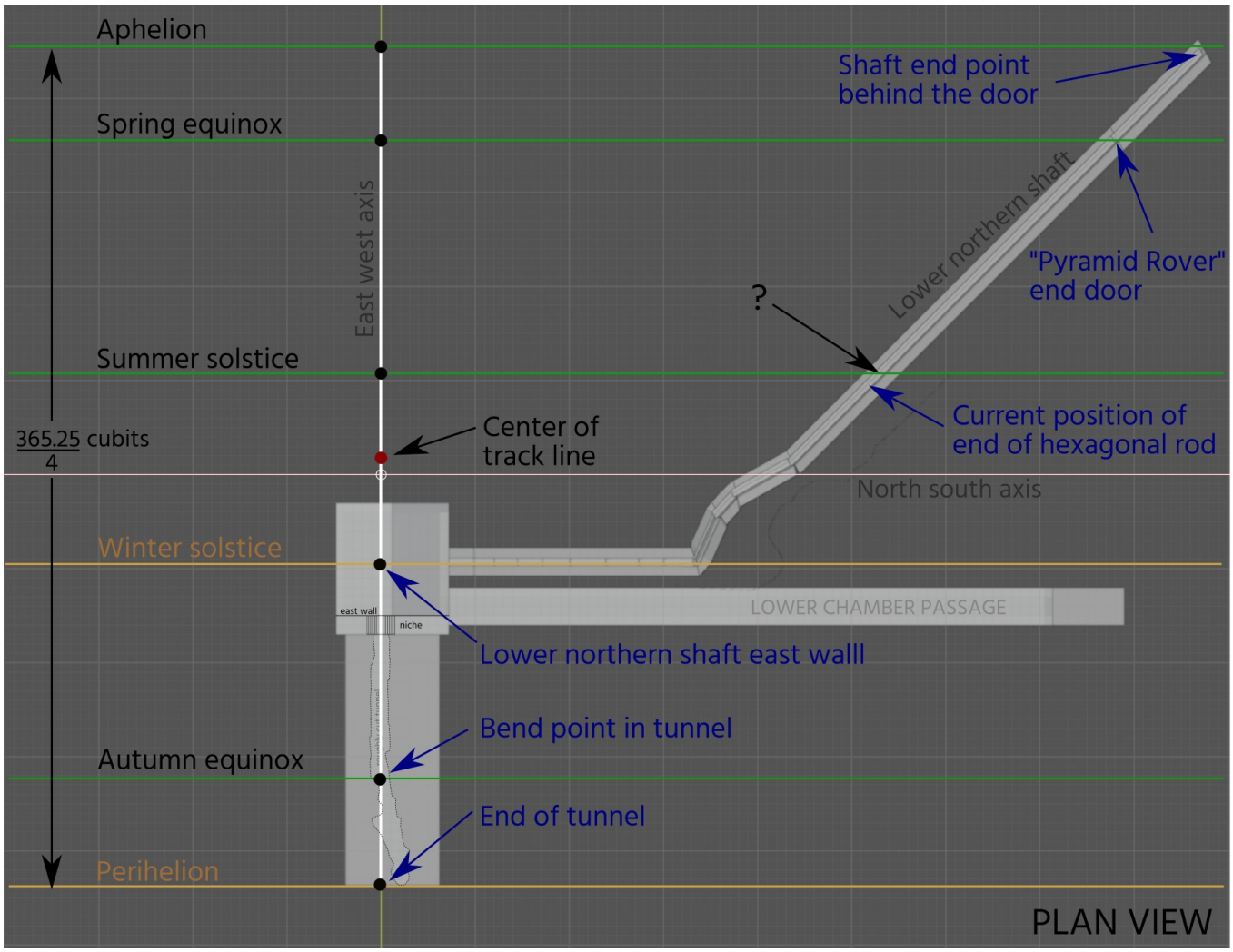

Diagram I-39 - A plan view of the annual astronomy events from NASA's DE441 marked along the Great Pyramid's east-west axis.

Diagram I-39 shows the same data points in plan view. All the ephemeris data points match up with the distinct locations within the architecture with the exception of one event, the summer solstice, which looks like it should match up with the top end of the hexagonal rod at the point on the diagram marked with a question mark, but doesn't by about 2 cubits. This is not a mistake in the calculations, it is a deliberate part of the architectural design which leads to the next part of the puzzle.

The reason for the offset is that the center point of the track line, which is also shown on the diagram, is situated about two cubits to the west of the central north-south axis of the pyramid and needs to be moved to the center point of the building as part of the solution. The initial position of the center of the track line is known mathematically from the previous calculations as being on the y-axis 1.971 cubits to the west of the origin, so the distance that the track line needs to be moved is known with precision.

As a result of this centering, the top of the hexagonal rod then aligns with the summer solstice line to well within the error margins of the distances reported by the Pyramid Rover team. Researching why the orbit track line needs centering was an involved process, and the answer lies in realising that the linear track line that has just been created is of no use unless it is accompanied by an elliptical orbit path around which the earth can move.

The earth orbit

Because the architects related the unit of the linear track line to time in days, making it 365.25 / 4 cubits long, and this track line length is about to be used to create the diameter of an orbit ellipse, they have multiplied the track line length by pi/2 when creating the orbit diameter, giving the semi major diameter of the orbit ellipse as 365.25 pi / 8 cubits or 143.43 cubits. Their choice in creating the orbit diameter involving radians is designed to deliberately define it as containing true anomaly angular values, with the track line containing mean anomalies. From the DE-441 information shown in diagram I-35 the instantaneous eccentricity of the orbit at the winter solstice 2728 BCE can be used initially, and the resulting orbit ellipse drawn into the 3D model of the building as shown in diagrams I-40 and I-41.

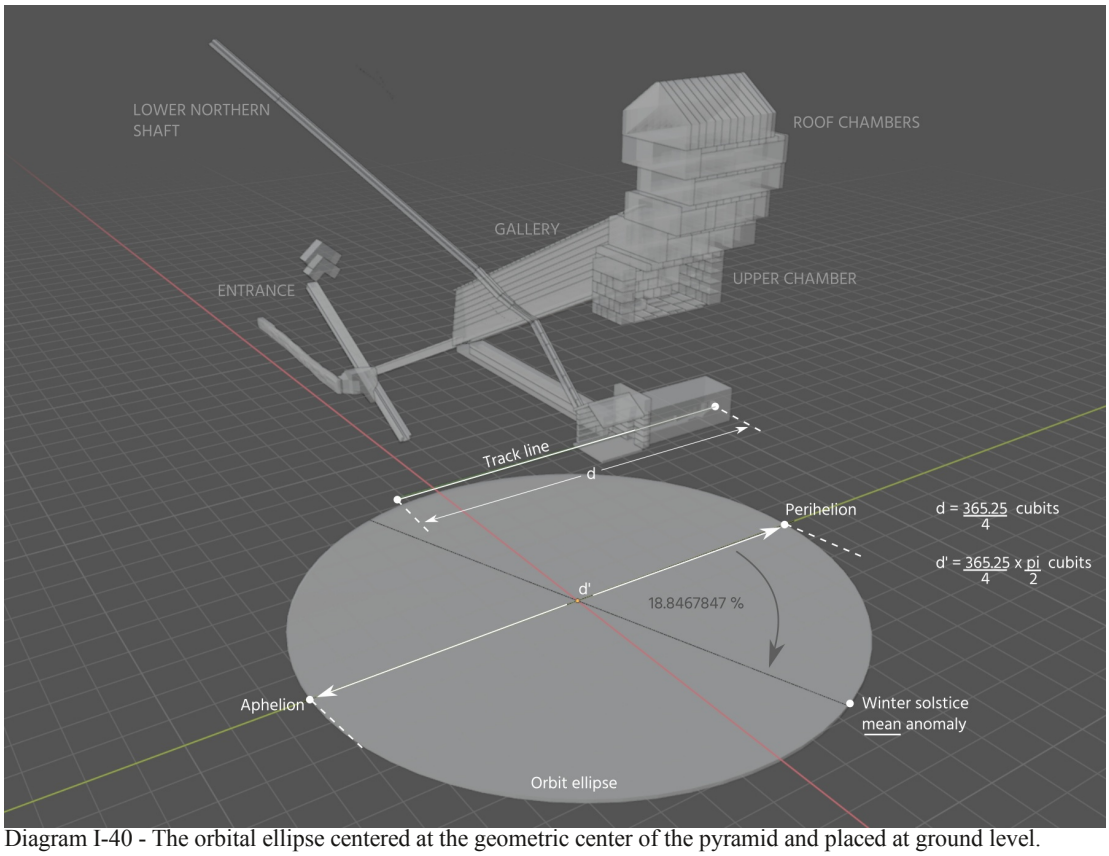

Diagram I-40 - The orbital ellipse centered at the geometric center of the pyramid and placed at ground level.

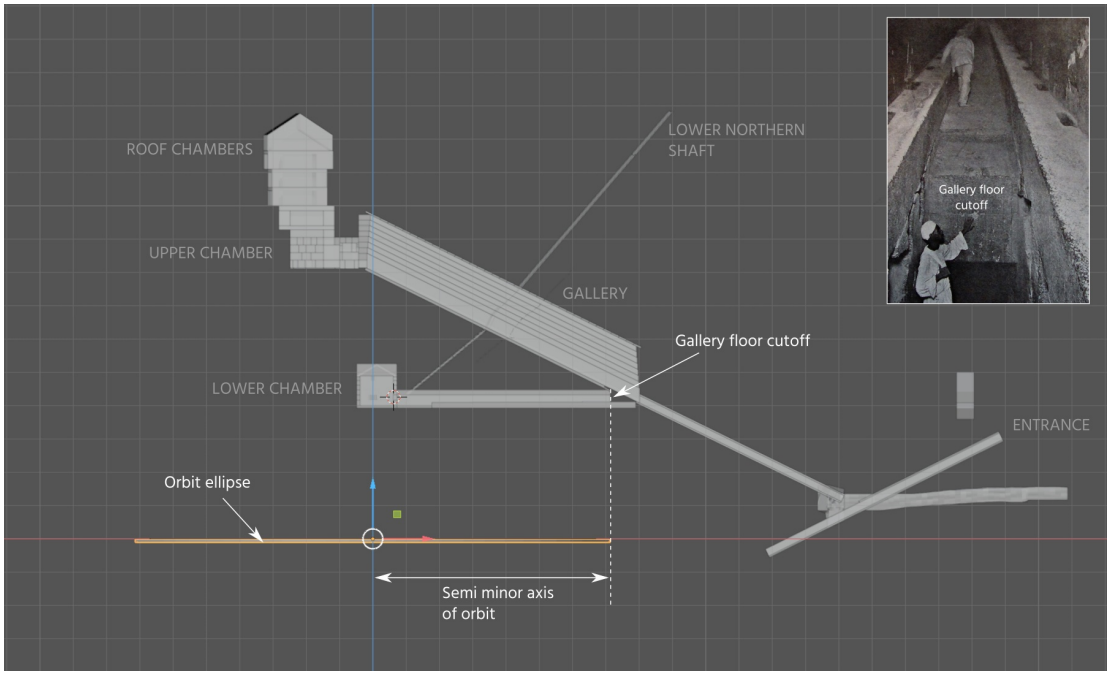

Diagram I-41 - The orbital ellipse viewed from the east in orthographic projection.

The cut off face of the gallery floor can be seen in diagram I-41 to be exactly aligned with the end point of the semi minor axis of the orbital ellipse, and this is the millimeter accurate defining geometry of what was always a curious part of the pyramid's design, and confirms the orbit has been correctly formed.

On diagram I-40 the winter solstice of BCE 2728 that was determined from the architecture is marked on the orbit as a *mean* anomaly, rather than a true anomaly, because at this stage this is the only piece of data that is available from the pyramid. The reason for marking this off in this manner is that there appears to be another piece of mathematics in the construction of the lower northern shaft that can be seen when viewing the orbit in plan view, as shown on diagram I-42.

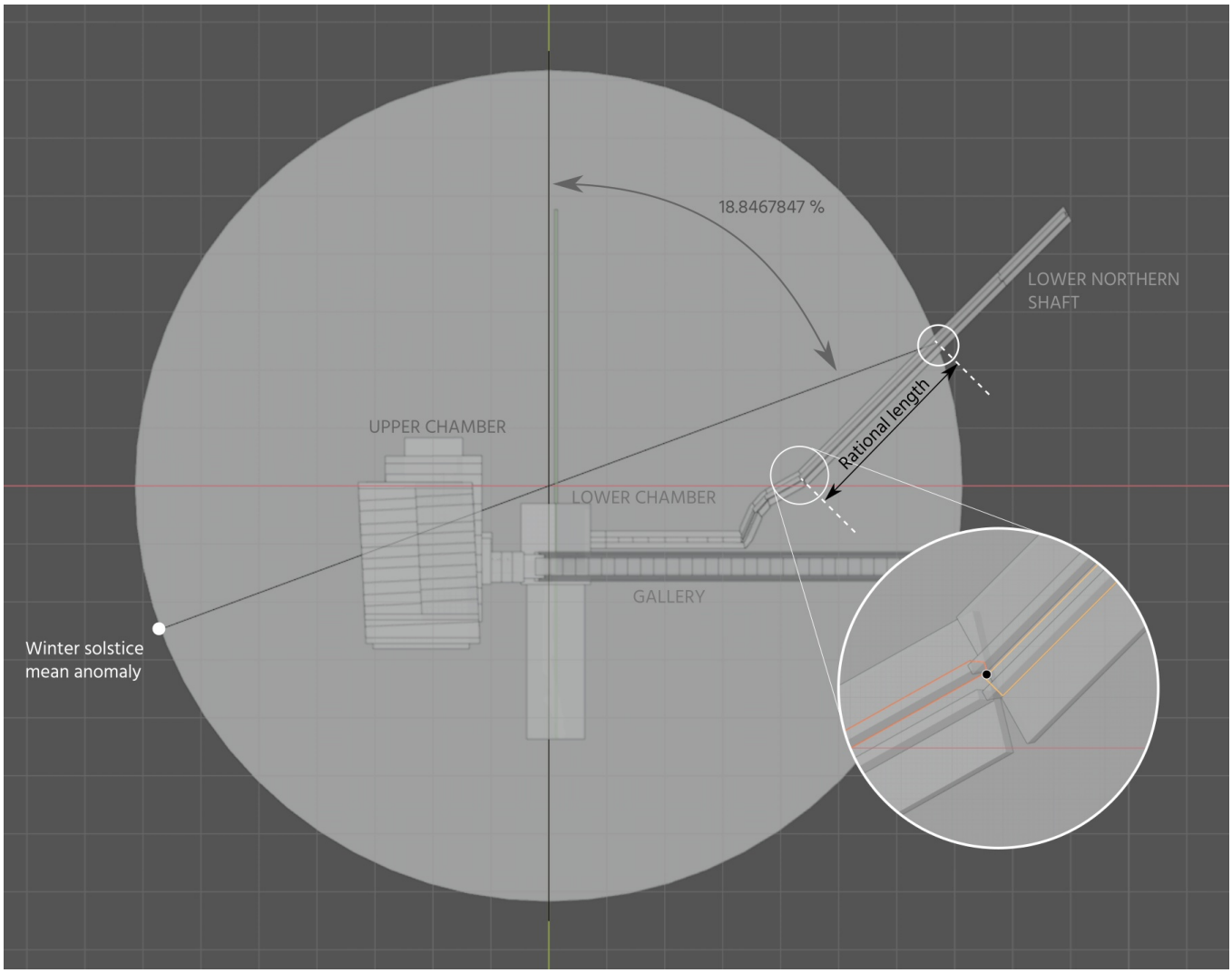

Diagram I-42 - The orbital ellipse viewed from above, showing the winter solstice alignment.

The lower northern shaft appears to be designed so that its west wall passes through the extension of the winter solstice line at a point on the orbital ellipse, and then the west wall joint between the fourth and fifth sections is a rational cubit length down the shaft from the orbit intersect point. The angle of this section of shaft has a 45 degree rotation around the z-axis, so if you know the exact details of the shaft's construction and the mean anomaly of the winter solstice from the architecture, then it should be possible to determine the exact location of the bottom of the fifth section of the shaft mathematically.

The reason that this location is important is that, as shown in diagram I-43, the west focus point of the orbit ellipse, which can be enumerated at this stage from the DE-441 data, aligns with the center of the shaft on the joint between the fourth and fifth sections. Because all of this system works from shifting the track line's center point to the pyramid origin, and that was only done because of the mismatch between the top end of the hexagonal rod and the summer solstice line, it can be concluded with absolute certainty that the hexagonal rod is an original part of the pyramid.

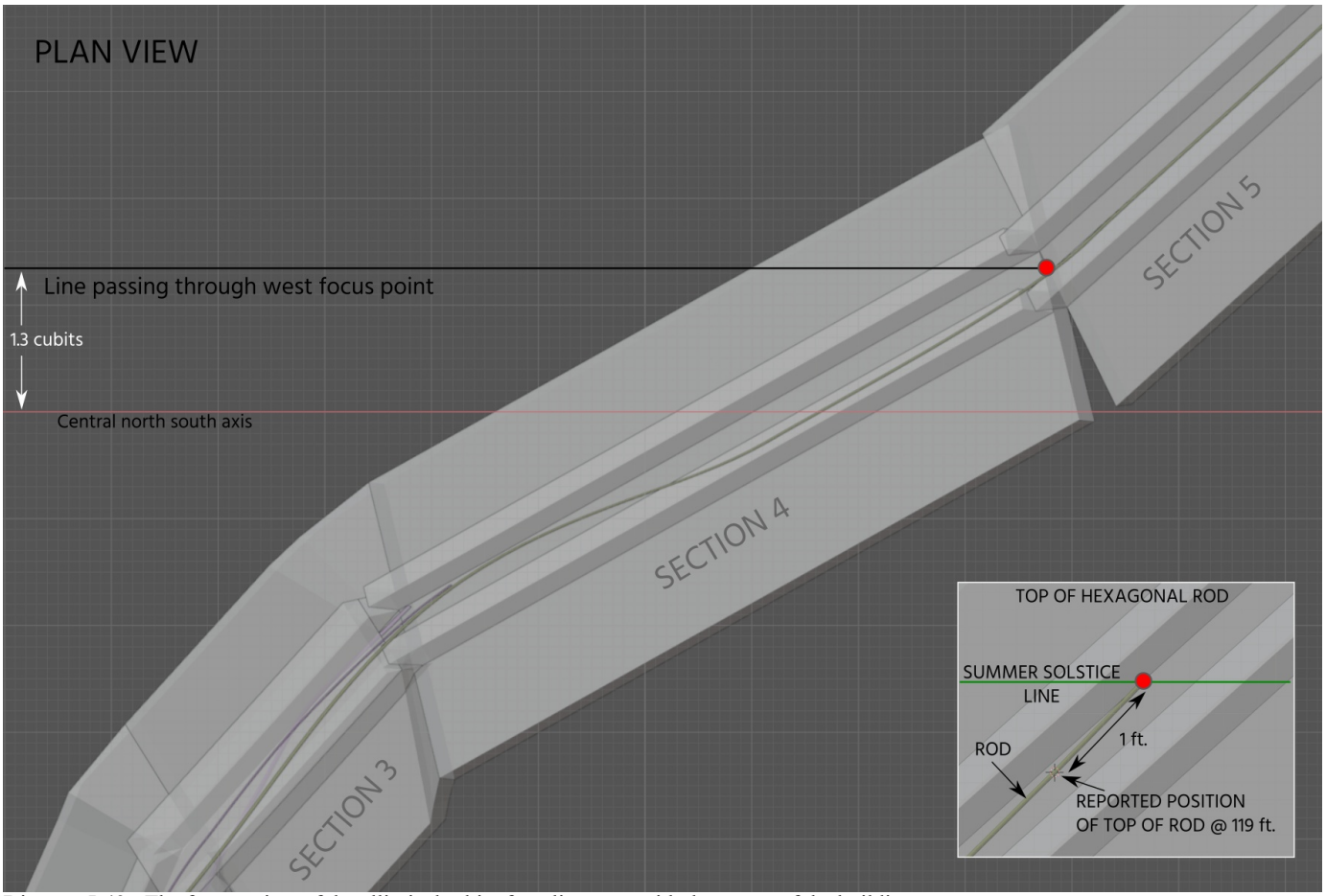

Diagram I-43 - The focus points of the elliptical orbit after alignment with the center of the building.

Summarising the previous four diagrams, the mathematics that requires solving to determine the Earth's orbit eccentricity is shown in diagram I-44 in which the location of the focus point of the ellipse needs to be adjusted, which then changes the eccentricity of the orbit, which then changes the intersect point on the orbit with the fixed winter solstice line, which then changes the position of the focus points of the ellipse.

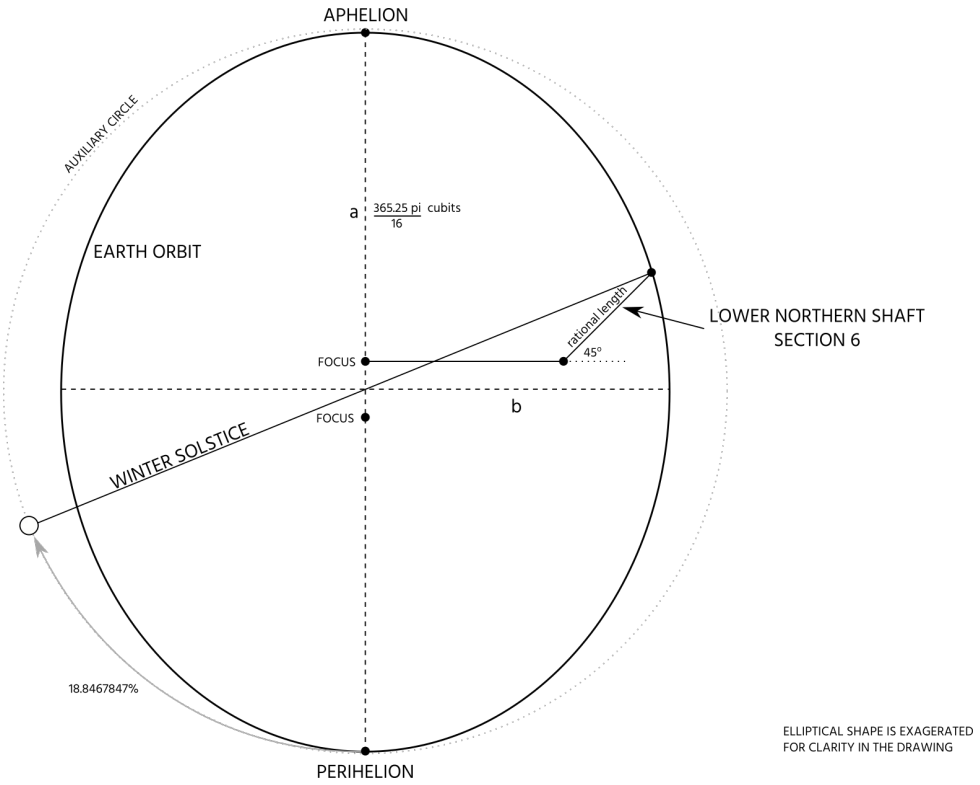

Diagram I-44 - The mathemematics of the earth's orbital eccentricity within the pyramid.

After significant time spent trying to find a solution to this mathematics problem it becomes apparent how the system has been designed. There is no solution that involves a rational length of shaft set at 45 degrees to north. It is the focal length of the ellipse that is the rational value and is exactly 1 and 1/3 cubits in length, and it is by trying to solve the problem outlined in diagram I-44 that this value for the focal length can be determined.

The orbital ellipse therefore has the following characteristics

Semi major axis	365.25 π /16	71.71666979523	(cubits)
Focal length		1.33333333	(cubits)
giving			
Eccentricity		0.01859167941207	
Semi minor axis		71.70427427107	(cubits)

The orbit's eccentricity can be compared against the value from the DE-441 ephemeris data for the 2728 BCE winter solstice which is given as 0.01855895171 which produces a difference in the orbit's semi minor axis between the pyramid value and the ephemeris value of 90km. The error between these two values is in the ephemeris data and not in the pyramid, due to the known inherent errors of the ephemeris.

It's now possible to calculate the true anomaly of the winter solstice from the pyramid data without having to refer to any ephemeris data, since we have the mean anomaly of 18.846% , or 67.84842°, and the orbit's eccentricity given to us for the winter solstice of 2728 BCE by the architects. The true anomaly of the winter solstice in BCE 2728 is 69.83866149 degrees.

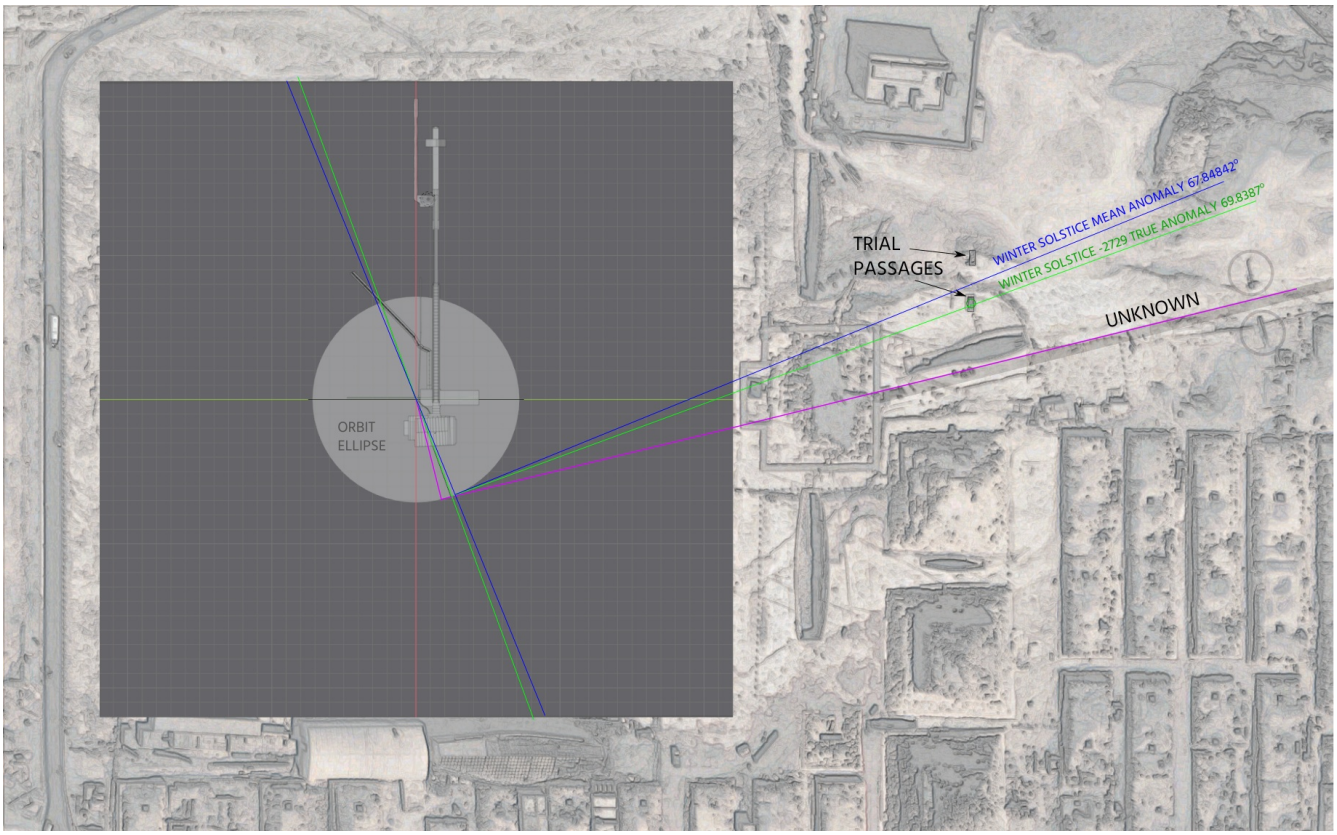

Diagram I-45 - The winter solstice and the start of the defining geometry of the causeway of the Great Pyramid of Giza.

Knowing the mean and true anomalies of the winter solstice 2728 BCE , it is possible to go outside the Great Pyramid and view the structure and geometry from above and identify how these data points align with features on the Giza plateau. As shown on diagram I-45, perpendiculars taken from the mean and true anomaly lines on the orbit emerge on the east side of the pyramid and pass through the area of the plateau where the trial passageways are situated.

Looking at other features on the plateau, what is immediately noticeable is that the north side of the main causeway to the pyramid forms a tangent to the orbit ellipse and this geometric alignment has been shown on diagram I-45 with the magenta line.

The tangent point on the orbit clearly is not the winter solstice, but by taking accurate measurements from the satellite image and then searching through the DE-441 data it is possible to pinpoint the true anomaly value of this tangent point on the ellipse and then see what is being represented. The answer is that the point on the elliptical orbit at which the difference between the true and mean anomalies is at its maximum falls on the Julian date JD 725042.44535821 BCE 2728-Jan-21 22:41:19 at a true anomaly of 75.824891^{o} and a mean anomaly of 73.747845^{o}, noting that this is now into the following year after the data in diagram I-35. These orbital positions can be accurately drawn onto the plan view of the plateau as shown on diagram I-46.

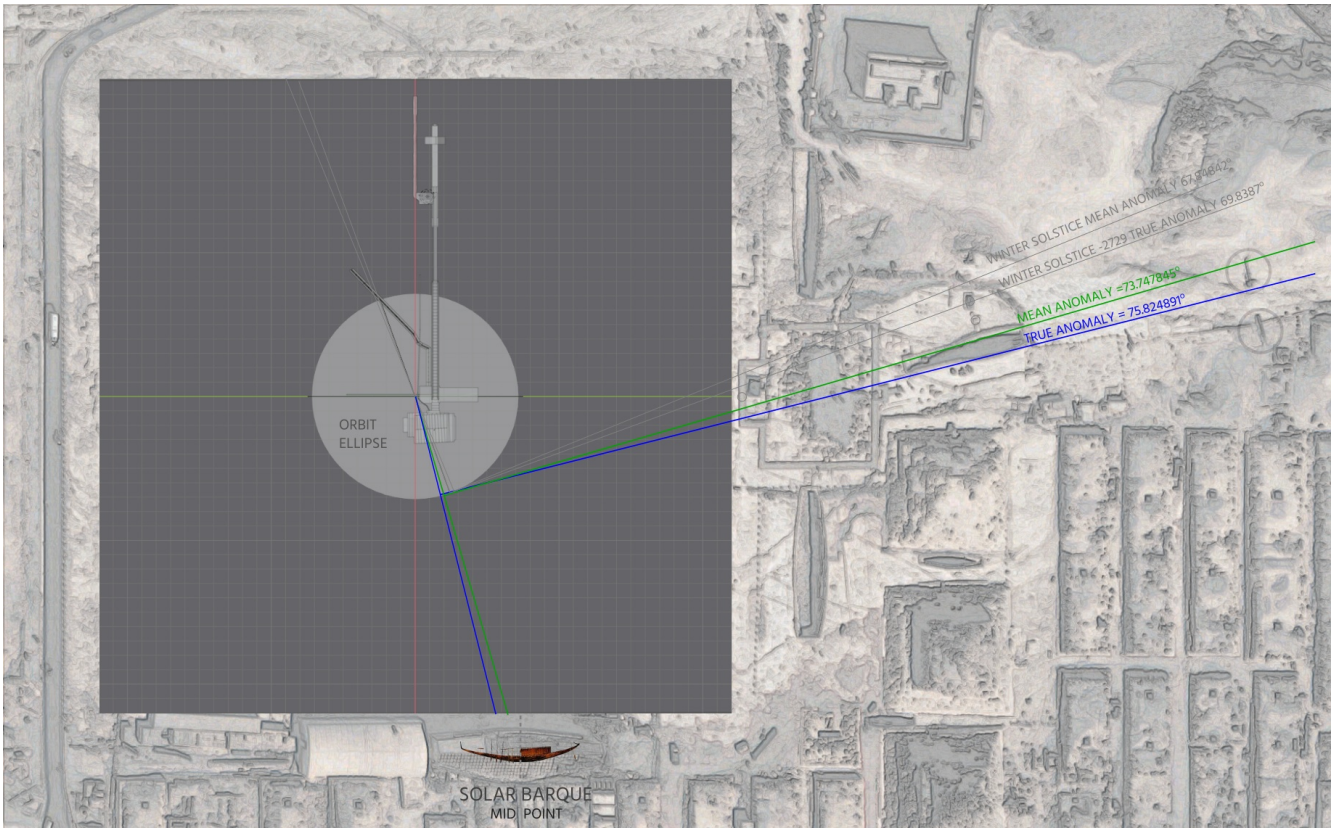

Diagram I-46 - The winter solstice and the start of the defining geometry of the causeway of the Great Pyramid of Giza.

Because it is the true anomaly that runs parallel to the main entrance causeway, the architects are showing in explicit terms that the orbital positions are indeed true anomaly values. The two walls that delimit the causeway, which are circled in grey on the satellite image are the same distance apart as the anomaly lines at that point, from which the design system can be understood. The date has been selected outside the range shown earlier because the principal of the system is being explained, and the data point on the orbit itself is being used only for that purpose. The reason that the point on the orbit is that of maximum difference between the mean and true anomalies is to show that in the dynamic system that is being created, the center of the elliptical orbit needs to traverse along the north-south axis of the pyramid as the true anomaly varies, whilst at the same time the date traverses along the east-west axis track line. The position of the south side of the causeway shows the maximum traversal along the east-west axis because it specifically uses the date of the maximum difference between the two anomalies as its defining line.

The traversal distance can be obtained from the lower chamber's architecture and is 365.25/20 cubits or 18.625 cubits, and diagram I-47 shows the maximum position of the movement of the earth orbit along the north-south axis 18.625 cubits to the south of the pyramid's center point.

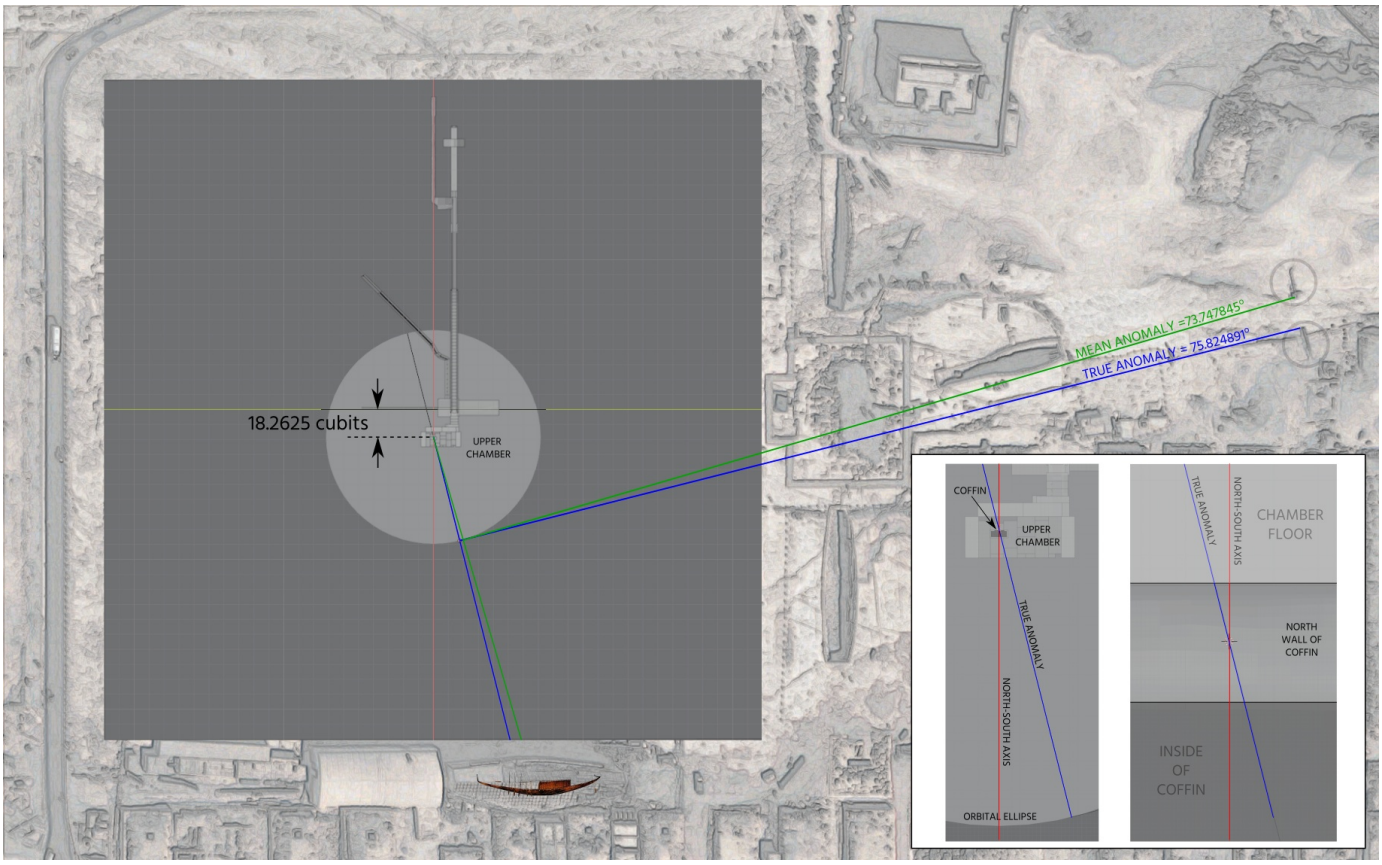

Diagram I-47 - The alignment geometry of the true and mean anomalies at maximum displacement south.

The true anomaly line is the angular defining line and matches up with the causeway's angle and the delimiting wall to the south of the causeway, with the mean anomaly line matching perfectly with the opposite northern wall of the causeway and running through the center of the pyramid temple door.

The inset illustrations in diagram I-47 show the alignment of the 18.625 cubit maximum traversal in the upper chamber aligning to the millimeter with the center of the north wall of the coffin, which was moved into this position in an earlier paper[12] following the logic of the stonework in the upper chamber walls. The system is complete and self-validates with previous parts of the pyramid's known architecture.

The start of the lower northern shaft

It is now possible to go back to the start of this paper and look once again at the unusual markings on the lower chamber wall around the opening in the north wall where the lower northern shaft commences.

There is one piece of data in the DE-441 ephemeris that stands out, and that is that the year between the winter solstice 2729 BCE and that of 2728 BCE was almost exactly 365.25 days long, which is quite unusual. Because of the interaction of the planets in the solar system and other dynamic elements such as the motion of the moon, the time that it takes the earth to traverse along its orbital path around the sun is never exactly one Julian year, 365.25 days, in length. To come across a time between consecutive winter solstice events of 365.249 Julian days is noticeable in the data, and it raises an interesting question.

The DE-441 ephemeris tables use two different time frames depending upon which data table you are accessing. For observational data the time frame is UT which is the standard Earth based time that is used in every day life, and if you access the osculating elements of the solar system the ephemeris uses a time frame called TDB or barycentric dynamic time. Simply put, this is the time that a clock would measure if placed at the center of the solar system, and it runs slower than clocks on Earth because of the effects of relativity. So there are two lengths of the year shown in diagram I-35, that measured in Earth based time

(JDUT) with a year length of 365.249145547 and solar system center based time (JDTDB) with a year length of 365.249477233. So that events from one ephemeris table can be matched up with events from the other, NASA has a column in the output of the observer data table which specifies TDB minus UT, which needs to be read along with the time it takes light to travel from an event happening in one place when seen from the other. In order to be able to understand the astronomy values that are being presented in the pyramid with confidence it is necessary to know which of the two time frames is being used, and the architects understood and solved this problem and wrapped it up in a *highly* complex wall puzzle. They have used the tiny difference between an average Julian year and the actual length of the winter solstice year in 2729 BCE and built this distance into the architecture.

The width of the piece of stone that blocks the left side of the entrance to the lower northern shaft is an amplified representation of the time difference between the winter solstice events for the year 2729 BCE and the following year 2728 BCE, and is calculated as shown in diagram I-48 which shows the architect's complex puzzle on the wall. The essence of the puzzle is that it uses two measurement units, the cubit (c) and the stack constant (n) and there is a horizontal line on the wall which is the same number of cubits vertically from the gable apex as it is stack constants vertically from the floor. Analysing the wall features that make up this puzzle on diagram I-48a and I-48b, the puzzle is comprised of

1) The gable height of the chamber, which was the first maths item encountered in the pyramid[13]
2) The heights of the wall stonework, noting that levels 4 and 5 need to be considered together when looking at the surveying, due to a non horizontal joint between them.
3) The height of the shaft opening, which requires mathematics knowledge of the first shaft bend construction, and the height of the shaft 2*n*
4) Levels zero and one of the stonework are both exactly 8*n* high
5) The stone insert in the wall to the left of the shaft opening is the lower portion of a triangle that reaches to the roof gable height.
6) The square area directly below the triangle has a side length of 1*n* at the start of the puzzle and is an iterative piece of mathematics, which is why it is shown as f(n) on the diagram.
7) The top of the north wall to the top of level zero is a logical value based on the 365.25 length of a year.

The two discontinuous line sections on the diagram I-4*8a* marked with the yellow asterisks have the required lines already marked on the wall by the architects and therefore additional illustration would only serve to cover up these lines, they are however continuous lines. The heights of each of the stone levels from surveying measurements is shown on diagram I-48b by the measurements in black on the north wall.

The method of solving the puzzle is as follows. The small quadrilateral below the triangle, marked with side lengths of f(*n*) and 1/f(*n*) starts out with a side length of 1*n* units, and is square. The height of this quadrilateral is increased until the distance in stack constants from the floor to the top of it is numerically equal to the distance from the gable apex to it in cubits. The width of the quadrilateral is at the same time decreased proportionally. When the balance point is reached the numerically equal lengths are 9.2388817 in respective units and the width of the quadrilateral, which is also the base length of the triangle above it, is 0.8071795 *n*. The tangent of the triangle's acute angle at the apex of the room can then be calculated from these two figures allowing the horizontal width of the triangle at any point to be determined.

The distance from the apex of the room to the floor of the shaft can be be calculated from the known information on diagram I-48 from which the width of the stone insert in the shaft entrance, at shaft floor level, can be calculated as 0.149184 cubits. This value can expressed in centicubits, following the architect's instructions from the upper chamber, as 14.9184 and be given the algebraic letter *q*.

The white dashed line that runs along level 1 of stonework and which marks of the top of the architect's

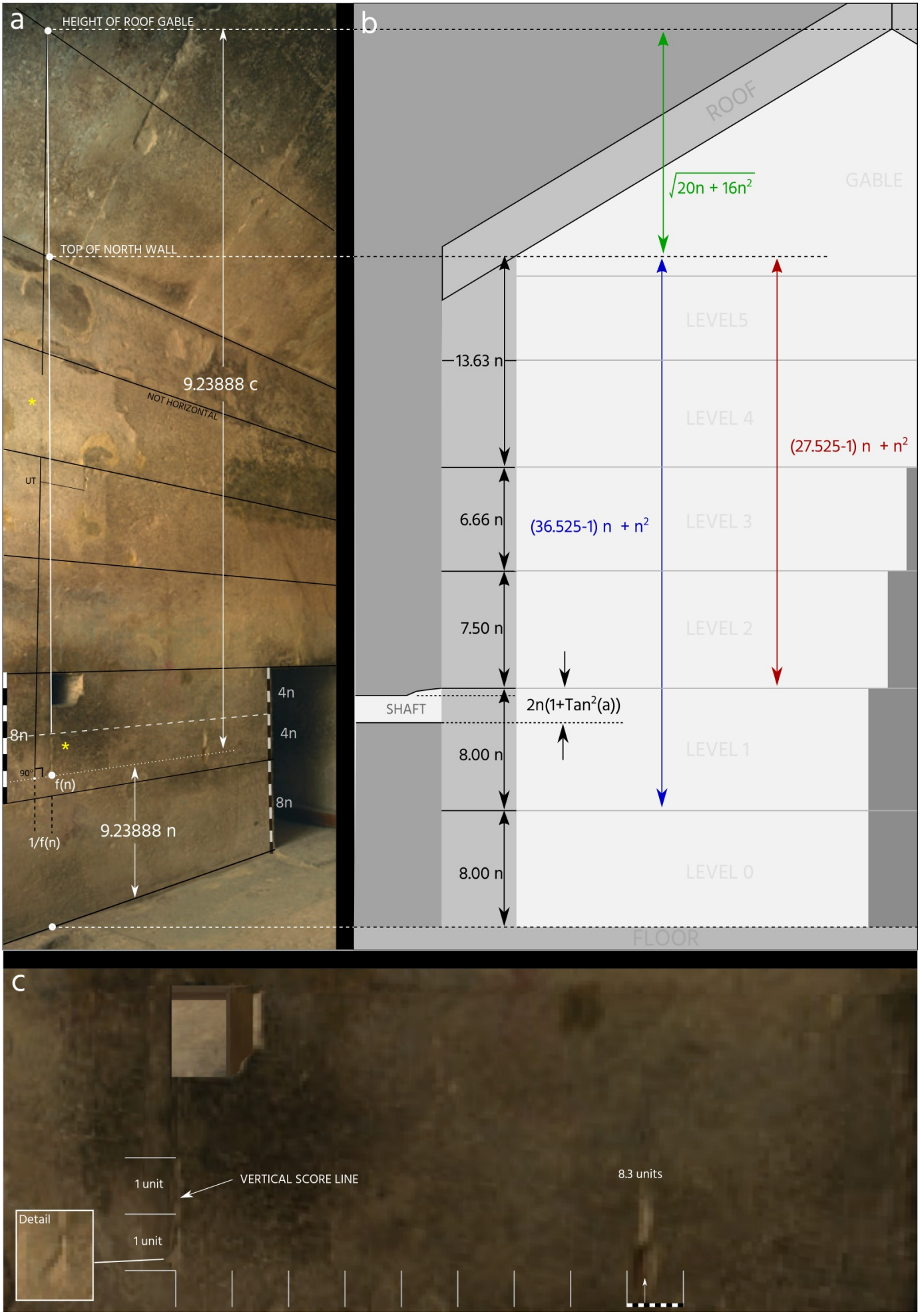

Diagram I-48 - The north wall of the lower chamber shown from a photo, technical drawing and 3D render.

vertical scored line in the triangle appears to be placed along the vertical center of this level of stones, 4 cubits from both the top and the bottom of the level, but isn't. There is a small, very precise, adjustment that needs to be made to its location, which is the equivalent of the checksums that were seen in the previous papers where the component parts of the calculations required up to this point are included at the last stage to ensure that you have correctly understood the system being used. The correct value for this distance from the top of the shaft entrance down to the top of the score line is

$$4 + n_x10^{-3} + \pi_x10^{-6} - q_x10^{-9}$$

There is now sufficient information to calculate the width of the stone insert at the level of the dashed white line as precisely 0.15505025618321 cubits. This value is the time difference between the year length in 2729 BCE and the average Julian year length, measured on the scale of the track line.

The length of the year along the linear track line of the Earth's movement has already been determined as being 365.25/2 cubits and so the width of the stone insert just calculated can be converted into Julian years , giving 0.000849 Julian years, giving the length of the year between the winter solstices of 2729 and 2728 BCE as 365.249150991235. This value can then be compared to the values in from the DE-441 ephemeris to determine the time frame being used :

Year length in the pyramid	365.249150991235
Year length DE-441 TDB	365.249145547
Year length DE-441 UT	365.249477233

The astonomy data in the architecture of the lower chamber is using a TDB time frame.

The architects have gone further to prove this point as shown in diagram I-48c.

The height of the vertical score line on the wall must be known with mathematical precision because its upper and lower bounds have been calculated. It has a length of 56.487761338 centicubits to which, as a check sum, the architects have added one centicubit and then used this value to represent two units of measure (in the same way that the earth track line shows 2 days of time for every 1 cubit of measure). The unit length shown by the score line is therefore exactly 0.287438806691367 cubits.

If the orbital ellipse was twice the size that has so far been calculated (making the linear track movement in a year equal to 365.25 cubits), then the ellipses semi-major axis length would be 365.25 π /8 cubits and dividing this axis length through by the unit measure just calculated results in the semi-major axis of the orbit as being 499.004783805926 of these units long.

This value can be compared to our current value for the definition of the 'Astronomical Unit' or *au* when measured in TDB light seconds of 499.004783805(81) and it can be seen that the unit defined by the score line is the light second, measured in a TDB time frame.

Diagram I-48c shows 2 of these units of measure against the score line from which the unit is defined, and also shows a horizontal measurement from the score line to a significant indentation on the wall which is 8.3 units in length, that being the distance from the earth to the sun in light minutes at the moment of the winter solstice 2728 BCE.

References

1. Gantenbrink, R. https://web.archive.org/web/20120305002107/http://www.cheops.org/startpage/thefindings/thefindingsn3.htm
2. Sibson, M. *Inside the Great Pyramid Queen's Chamber Northern Shaft* https://www.youtube.com/watch?v=Ki0405ulvIY
3. Brabin, S.H. *Decoding the north and west walls of the upper chamber of the Great Pyramid*, ISBN 978--09566588-6-9 https://www.giza-pyramids.com/documents/pdf/GPP_E-DecodingTheUpperChamber1.pdf
4. British Museum, Spherical dolerite pounder https://www.britishmuseum.org/collection/object/Y_EA67818
5. Hawass, Z. *The so-called secret doors inside Khufu's pyramid* 43rd edition of the Supplément aux Annales du Service des antiquités de l'Egypte, page 58
6. Hawass, Z. *The National Geographic / Supreme Council of Antiquities Scientific Expedition Final Report* 20 December 2002 page 21
7. Brabin, S.H. *The Lower Northern Shaft* http://www.giza-pyramids.com/HTML_Pyramid/C/C10_lower_northern_2.html
8. Brabin, S.H. *The Great Pyramid, the Earth and the Cubit*, ISBN 978-0-9566588-8-3 https://www.giza-pyramids.com/documents/pdf/GPP_G-TheEarthModel.pdf
9. Laskar, J. (1986). *Secular terms of classical planetary theories using the results of general theory* Astronomy and Astrophysics. 157 (1): pages 59–70.
10. V.Maragioglio and C.Rinaldi *L'Architettura delle piramidi menfite*, Torino, 1963. Parte IV Plate 6
11. Brabin, S.H., *The horizontal chamber stack of the Great Pyramid* https://www.giza-pyramids.com/documents/pdf/GPP_C-HorizontalChamberStack.pdf, page 10 dig. C9
12. Brabin, S.H. *Decoding the north and west walls of the upper chamber of the Great Pyramid*, ISBN 978- 0-9566588-6-9 http://www.giza-pyramids.com/documents/pdf/GPP_E-DecodingTheUpperChamber1.pdf , Page 11
13. Brabin, S.H. *The vertical chamber stack of the Great Pyramid part 1* ISBN 978-0-9566588-3-8 http://www.giza-pyramids.com/documents/pdf/GPP_B-VerticalChamberStack1.pdf , Page 5